

Histological Assessment of Cartilage Repair

According to the International Cartilage Repair Society (ICRS) (Mainil-Varlet et al. 2003), microscopic findings were evaluated by two examiners in a blind manner, using HE- and Safranin-O–stained sections. ICRS proposed six categories with individual scores, which are described in the legend of Table 1.

Statistical Analysis

All analyses were performed using Student's *t*-test or the Mann-Whitney U-test, as indicated in the figure and table legends (StatView J-5.0; SAS Institute, Cary, NC). Data are presented as the means \pm SE. Differences were considered significant when $p < 0.05$.

Results

Microscopic Evaluation of Cartilage Repair

We transplanted osteochondral grafts obtained from EGFP-expressing rats into the cartilage of wild-type rats. At 1, 2, or 4 weeks after transplantation, no apparent macroscopic difference was observed between PTD-FNK treatment and non-treatment groups; however, HE and Safranin-O/Fast Green staining showed microscopic differences between them, as mentioned below.

At 1 week, a significant difference appeared in cell distribution (Table 1). All graft cartilage without PTD-FNK treatment showed abnormal cell distribution, that is, a mixed pattern of columnar arrangement and cluster of chondrocytes (Figures 1A and 1B; Table 1). On the other hand, chondrocytes were arranged in a columnar pattern in the PTD-FNK treatment group (Figures 1D and 1E; Table 1). In both groups, we observed slightly irregular surfaces (Figures 1A and 1D; Table 1) and necrosis in the subchondral bone to the same extent (Figures 1C and 1F; Table 1). The other features were almost normal, although one graft without PTD-FNK treatment showed low cell population viability (Figure 1B; Table 1) and low-level Safranin-O staining (matrix) (Table 1).

At 2 weeks, grafts with PTD-FNK treatment seemed to be slightly better than grafts without PTD-FNK treatment with regard to cartilage surface and cell distribution (Figures 1G and 1H; Table 1). It is noted that one graft without PTD-FNK treatment formed chondrocyte clusters (Figure 1H; Table 1). We also observed increased remodeling of subchondral bone in both groups (Figures 1I and 1L; Table 1).

At 4 weeks, cartilage surfaces of both groups were slightly irregular; however, there was another significant difference in the matrix between the two groups (Table 1). All graft cartilage with PTD-FNK treatment showed almost normal matrix (Figure 1Q), whereas the cartilage of two grafts (50%) without PTD-FNK

treatment was found to be fibrocartilage, which developed just above the tidemark (Figure 1N). In addition, PTD-FNK treatment seemed to suppress deterioration of cell distribution but not to increase cell population viability (Table 1). There was no difference in the subchondral bone and cartilage mineralization of either group (Figures 1O and 1R; Table 1).

Microscopic assessment strongly suggested that PTD-FNK suppresses a matrix deterioration and disruption of columnar chondrocyte distribution during the study period.

Safranin-O/Fast Green Staining

Safranin-O stoichiometrically binds to tissue glycosaminoglycan, such as chondroitin sulfate and keratan sulfate (Rosenberg 1971), and is widely used to evaluate the amount of proteoglycan present in cartilage (Mainil-Varlet et al. 2003). Safranin-O/Fast Green staining allowed us to be aware of another important finding. Grafted cartilage exhibited high-level Safranin-O staining at 1 and 2 weeks in both groups (Figures 1B, 1E, and 1K). At 4 weeks, no great difference in the intensity of Safranin-O staining was observed between the graft and host cartilages; however, all cartilage layers of grafts with PTD-FNK treatment remained Safranin-O staining positive through almost the entire thickness (Figure 2). In contrast, the cartilage layers of grafts without PTD-FNK treatment showed a significant reduction of Safranin-O staining in the superficial

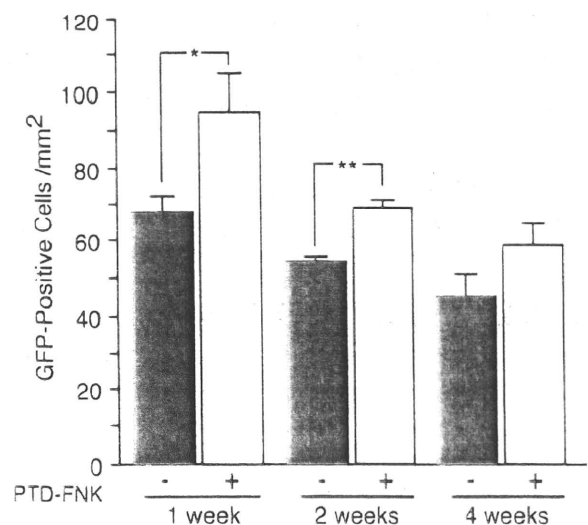


Figure 4 A number of EGFP-positive cells were normalized against the area of the cartilage layer (surviving cell density). PTD-FNK significantly suppressed a decrease in EGFP-positive cells at 1 and 2 weeks, and the tendency seemed to be continuing at 4 weeks. * $p < 0.05$ and ** $p < 0.001$ vs the PTD-FNK non-treatment group at 1 or 2 weeks by Student's *t*-test.

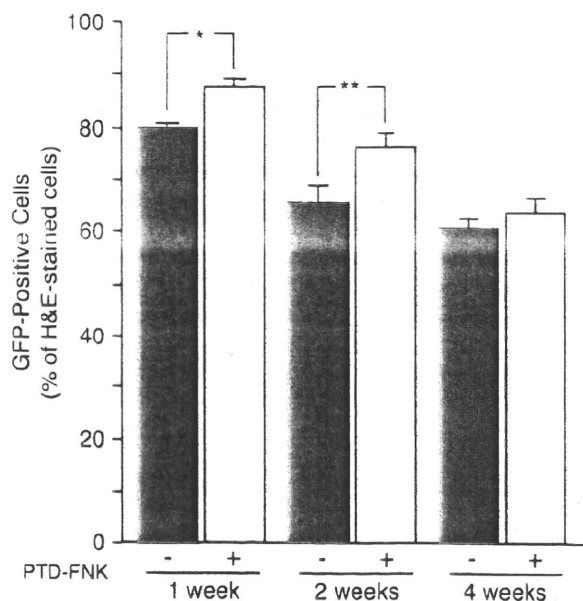


Figure 5 The number of EGFP-positive cells normalized against a number of hematoxylin-eosin-stained cells (survival rate) showed that PTD-FNK protected from cell death at 1 and 2 weeks, and the tendency seemed to be continuing at 4 weeks. * $p < 0.005$ and ** $p < 0.005$ vs PTD-FNK non-treatment groups at 1 or 2 weeks by Student's *t*-test.

zone, indicating that some chondrocytes, but not all, lost their activity to synthesize glycosaminoglycan. Analysis with NIH Image Soft ware showed that the superficial zone losing Safranin-O staining in the PTD-FNK untreated group was ~10 times thicker than that in the PTD-FNK treatment group (Figure 2). PTD-FNK clearly suppressed the loss of Safranin-O staining for 4 weeks, indicating that PTD-FNK preserves chondrocytes from losing cellular activity to maintain normal proteoglycan for at least for 4 weeks.

Chondrocyte Survival

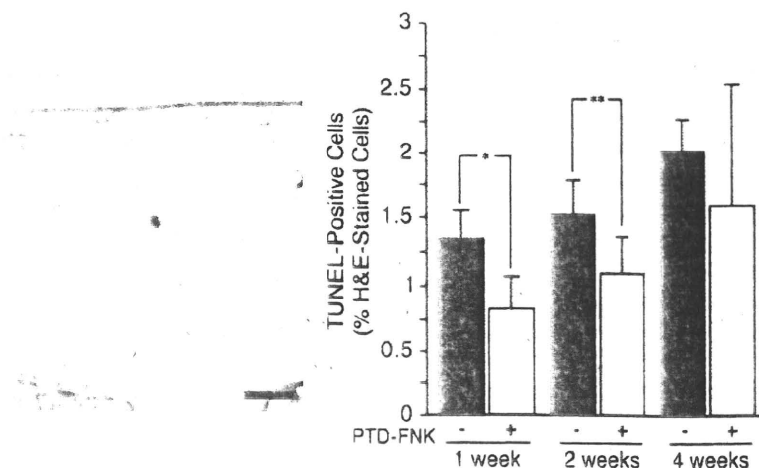
Microscopic assessment of cartilage suggested that the PTD-FNK treatment group obtained higher scores of "cell distribution" at 1 week and "matrix" at 4 weeks, but there was no difference in the category "cell population viability" during the study period. The category "cell population viability" was roughly evaluated by the morphology of HE-stained cells and nuclei (e.g., pyknotic nuclei in a dying or dead cell) (Mainil-Varlet et al. 2003); therefore, the evaluation is not quantitative. To study the survival effect of PTD-FNK on chondrocytes in grafts, EGFP-positive cells in the cartilage layer of grafts were counted, because surviving chondrocytes of osteochondral grafts prepared from SD-Tg (CAG-EGFP) rats expressed EGFP during the study period (Figure 3).

The number of EGFP-positive cells was normalized against the area of the cartilage layer (Figure 4). PTD-FNK significantly suppressed a decrease in EGFP-positive cells at 1 and 2 weeks, and the tendency seemed to continue at 4 weeks. The number of EGFP normalized against the number of HE-stained cells also showed that PTD-FNK protected against cell death, although the difference was smaller (Figure 5). To evaluate dying or dead cells, TUNEL staining was performed. The results showed that PTD-FNK inhibited cell death (Figure 6), conforming to the above results. These results indicate that PTD-FNK protects chondrocytes from cell death caused by transplantation.

Discussion

This study showed that the degeneration of cylindrical osteochondral autografts, which were transplanted into the full thickness of articular cartilage defects by impact insertion, was suppressed when they were submerged in anti-cell death PTD-FNK protein before transplantation. Furthermore, the increased cell death

Figure 6 PTD-FNK inhibited cell death. Representative section of terminal deoxynucleotidyl transferase (TdT)-mediated deoxyuridine triphosphate (dUTP)-nick end-labeling staining (left). PTD-FNK significantly inhibited cell death at 1 and 2 weeks, and a similar tendency was found at 4 weeks (right). * $p < 0.05$ and ** $p < 0.005$ vs PTD-FNK non-treatment groups at 1 or 2 weeks by Student's *t*-test.



and decreased survival rate and density of GFP-positive graft cells, which occurred with time in the early stage after transplantation, were also suppressed in grafts treated with PTD-FNK.

PTD-FNK has been shown to inhibit cell death pathologically caused in various tissues, including the brain and liver, and caused by bone marrow transplantation and freezing/thawing, as mentioned above (Asoh and Ohta 2008). This study showed that the density and survival rate of the GFP-positive cells of PTD-FNK-treated grafts were significantly higher than those of PTD-FNK-untreated grafts but decreased with time during the study period. In the previous study, PTD-FNK was shown to be introduced into the chondrocytes from the superficial layer to a depth of 200 μm after 6 hr, when the cartilage slice was submerged in a solution containing PTD-FNK *in vitro* (Ozaki et al. 2004). The microenvironment of a cylindrical osteochondral graft, for example, blood supply to the subchondral bone and metabolism, and nutrition of the cartilage, is not the same as that of normal articular cartilage. In particular, in the early period after transplantation, horizontal mechanical stress on grafts decreases and the biological contact of subchondral bone between graft and host is lost, which generates an abnormal mechanical environment in the grafts; therefore, some environmental changes could cause chondrocyte death in grafts, regardless of PTD-FNK treatment. However, these results suggest that more chondrocytes were protected from cell death by PTD-FNK treatment at 1 and 2 weeks, resulting in matrix with a histologically normal appearance at 4 weeks.

PTD-FNK was degraded with a half-span of ~ 2 hr when introduced into a cultured cell (Asoh et al. 2002); PTD-FNK was degraded with a half-span of 3.6 or ~ 2 hr when systemically delivered into the brain or liver, respectively (Asoh et al. 2005; Katsura et al. 2008). Despite the short half-span of PTD-FNK in a cell, the cytoprotective effect of PTD-FNK obviously continued for at least 2 weeks when introduced into chondrocytes in cartilage. It is unlikely that PTD-FNK is very slowly degraded in chondrocytes. Meanwhile, chondrocytes are embedded in the cartilage matrix, which is rich in chondroitin sulfate containing high levels of sulfate with a negative charge. It is expected that chondroitin sulfate electrostatically interacts with PTD-FNK, because the PTD is rich in positively charged amino acid residues. It is possible that the matrix functions as a reservoir to store and supply PTD-FNK in the long term. PTD-FNK may gradually be dissociated from matrix components and introduced into chondrocytes. Otherwise, PTD-FNK exhibits cytoprotective activity only on the first day or for the first several days after transplantation, which may simply result in better survival of the cells

at 1 and 2 weeks. Further effort is necessary to improve the survival of chondrocytes and the properties of cylindrical osteochondral grafts for hyaline cartilage. Strategies are also sought to enhance the transduction of PTD-FNK to the subchondral bone because there was no histological difference in this area between PTD-FNK-treated and untreated grafts.

It remains unknown how PTD-FNK protects chondrocytes from mechanical stress during preparation and impact insertion of the graft. Recently, we showed that PTD-FNK inhibits an increase in the cytosolic calcium concentration induced by glutamate, thapsigargin, and an immunosuppressant, FK506, and protected primary cultured neocortical neurons and neuroblastoma cells from cell death (Asoh et al. 2002; Katsura et al. 2008). It is widely accepted that disruption of the regulation of intracellular calcium concentration leads to cell death (Giorgi et al. 2008). How do chondrocytes in cartilage respond to mechanical stress? Several studies showed that mechanical stress transiently induces an increase in intracellular calcium concentration in primary cultured chondrocytes (Guilak et al. 1999; D'Andrea et al. 2000; Kono et al. 2006). Mechanical stress also induced ATP release from chondrocytes to the extracellular matrix (Hatori et al. 1995), and direct ATP application to rat cartilage slices induced transient elevation of intracellular calcium concentration (Kumashashi et al. 2004). Recently, Huser and colleagues (2006,2007) reported that a single impact load induces a release of calcium from the endoplasmic reticulum, causing mitochondrial depolarization and caspase-9 activation resulting in apoptosis-like cell death of chondrocytes in cartilage within 24–48 hr. It is possible that PTD-FNK prevents the increase of intracellular calcium ions induced by mechanical stress and protects the chondrocytes from cell death. Further study remains necessary to investigate the mechanisms by which PTD-FNK protects chondrocytes from cell death associated with cylindrical osteochondral graft transplantation.

In conclusion, we present the efficacy of PTD-FNK to protect from cell death and suppress the degeneration of cylindrical osteochondral grafts. The histological score was well maintained, and the survival rate and density of GFP-positive cells were predominant in PTD-FNK-treated grafts; therefore, the potential of antiapoptotic protein PTD-FNK to suppress the degeneration of cylindrical osteochondral autograft was shown.

Literature Cited

- Arakawa M, Yasutake M, Miyamoto M, Takano T, Asoh S, Ohta S (2007) Transduction of anti-cell death protein FNK protects isolated rat hearts from myocardial infarction induced by ischemia/reperfusion. *Life Sci* 80:2076–2084

- Asoh S, Mori T, Nagai S, Yamagata K, Nishimaki K, Miyato Y, Shidara Y, et al. (2005) Zonal necrosis prevented by transduction of the artificial anti-death FNK protein. *Cell Death Differ* 12:384-394
- Asoh S, Ohsawa I, Mori T, Katsura K, Hiraide T, Katayama Y, Kimura M, et al. (2002) Protection against ischemic brain injury by protein therapeutics. *Proc Natl Acad Sci USA* 99:17107-17112
- Asoh S, Ohta S (2008) PTD-mediated delivery of anti-cell death proteins/peptides and therapeutic enzymes. *Adv Drug Deliv Rev* 60:499-516
- Asoh S, Ohtsu T, Ohta S (2000) The super anti-apoptotic factor Bcl-xL/NK constructed by disturbing intramolecular polar interactions in rat Bcl-xL. *J Biol Chem* 275:37240-37245
- Bobic V (1996) Arthroscopic osteochondral autograft transplantation in anterior cruciate ligament reconstruction: a preliminary clinical study. *Knee Surg Sports Traumatol Arthrosc* 3:262-264
- Borazjani BH, Chen AC, Bae WC, Patil S, Sah RL, Firestein GS, Bugbee WD (2006) Effect of impact on chondrocyte viability during insertion of human osteochondral grafts. *J Bone Joint Surg Am* 88:1934-1943
- Brandt KD (1987) Nonsteroidal antiinflammatory drugs and articular cartilage. *J Rheumatol* 14:132-133
- Buckwalter JA, Ehrlich MG, Armstrong AL, Mankin HJ (1987) Electron microscopic analysis of articular cartilage proteoglycan degradation by growth plate enzymes. *J Orthop Res* 5:128-132
- Chen CT, Burton-Wurster N, Borden C, Hueffer K, Bloom SE, Lust G (2001) Chondrocyte necrosis and apoptosis in impact damaged articular cartilage. *J Orthop Res* 19:703-711
- Chen H, Zhang L, Jin Z, Jin E, Fujiwara M, Ghazizadeh M, Asoh S, et al. (2007) Anti-apoptotic PTD-FNK protein suppresses lipopolysaccharide-induced acute lung injury in rats. *Exp Mol Pathol* 83:377-384
- D'Andrea P, Calabrese A, Capozzi I, Grandolfo M, Tonon R, Vittur F (2000) Interstitial Ca²⁺ waves in mechanically stimulated articular chondrocytes. *Biorheology* 37:75-83
- Dew TL, Martin RA (1992) Functional, radiographic, and histologic assessment of healing of autogenous osteochondral grafts and full-thickness cartilage defects in the talus of dogs. *Am J Vet Res* 53:2141-2152
- D'Lima DD, Hashimoto S, Chen PC, Colwell CW Jr, Lotz MK (2001) Impact of mechanical trauma on matrix and cells. *Clin Orthop Relat Res* 391(suppl):S90-S99
- Giorgi C, Romagnoli A, Pinton P, Rizzuto R (2008) Ca²⁺ signaling, mitochondria and cell death. *Curr Mol Med* 8:119-130
- Gomar-Sancho F, Orquin EG (1987) Repair of osteochondral defects in articular weightbearing areas in the rabbit's knee. The use of autologous osteochondral and meniscal grafts. *Int Orthop* 11:65-69
- Guilak F, Zell RA, Erickson GR, Grande DA, Rubin CT, McLeod KJ, Donahue HJ (1999) Mechanically induced calcium waves in articular chondrocytes are inhibited by gadolinium and amiloride. *J Orthop Res* 17:421-429
- Hangody L, Kish G, Karpati Z, Szerb I, Udvarhelyi I (1997) Arthroscopic autogenous osteochondral mosaicplasty for the treatment of femoral condylar articular defects. A preliminary report. *Knee Surg Sports Traumatol Arthrosc* 5:262-267
- Harman BD, Weeden SH, Lichota DK, Brindley GW (2006) Osteochondral autograft transplantation in the porcine knee. *Am J Sports Med* 34:913-918
- Hatori M, Teixeira CC, Debolt K, Pacifici M, Shapiro IM (1995) Adenine nucleotide metabolism by chondrocytes in vitro: role of ATP in chondrocyte maturation and matrix mineralization. *J Cell Physiol* 165:468-474
- Horas U, Pelinkovic D, Herr G, Aigner T, Schnettler R (2003) Autologous chondrocyte implantation and osteochondral cylinder transplantation in cartilage repair of the knee joint. A prospective, comparative trial. *J Bone Joint Surg Am* 85:185-192
- Hui JH, Chen F, Thambyah A, Lee EH (2004) Treatment of chondral lesions in advanced osteochondritis dissecans: a comparative study of the efficacy of chondrocytes, mesenchymal stem cells, periosteal graft, and mosaicplasty (osteochondral autograft) in animal models. *J Pediatr Orthop* 24:427-433
- Huntley JS, Bush PG, McBirnie JM, Simpson AH, Hall AC (2005) Chondrocyte death associated with human femoral osteochondral harvest as performed for mosaicplasty. *J Bone Joint Surg Am* 87:351-360
- Huser CA, Davies ME (2007) Calcium signaling leads to mitochondrial depolarization in impact-induced chondrocyte death in equine articular cartilage explants. *Arthritis Rheum* 56:2322-2334
- Huser CA, Peacock M, Davies ME (2006) Inhibition of caspase-9 reduces chondrocyte apoptosis and proteoglycan loss following mechanical trauma. *Osteoarthritis Cartilage* 14:1002-1010
- Kashio A, Sakamoto T, Suzukawa K, Asoh S, Ohta S, Yamasoba T (2007) A protein derived from the fusion of TAT peptide and FNK, a Bcl-x(L) derivative, prevents cochlear hair cell death from aminoglycoside ototoxicity in vivo. *J Neurosci Res* 85:1403-1412
- Katsura K, Takahashi K, Asoh S, Watanabe M, Sakurazawa M, Ohsawa I, Mori T, et al. (2008) Combination therapy with transductive anti-death FNK protein and FK506 ameliorates brain damage with focal transient ischemia in rat. *J Neurochem* 106:258-270
- Kleemann RU, Schell H, Thompson M, Epari DR, Duda GN, Weiler A (2007) Mechanical behavior of articular cartilage after osteochondral autograft transfer in an ovine model. *Am J Sports Med* 35:555-563
- Kono T, Nishikori T, Kataoka H, Uchio Y, Ochi M, Enomoto K (2006) Spontaneous oscillation and mechanically induced calcium waves in chondrocytes. *Cell Biochem Funct* 24:103-111
- Kumahashi N, Ochi M, Kataoka H, Uchio Y, Kakimaru H, Sugawara K, Enomoto K (2004) Involvement of ATP, increase of intracellular calcium and the early expression of c-fos in the repair of rat fetal articular cartilage. *Cell Tissue Res* 317:117-128
- Mainil-Varlet P, Aigner T, Brittberg M, Bullough P, Hollander A, Hunziker E, Kandel R, et al., International Cartilage Repair Society (2003) Histological assessment of cartilage repair: a report by the Histology Endpoint Committee of the International Cartilage Repair Society (ICRS). *J Bone Joint Surg Am* 85:45-57
- Makino T, Fujioka H, Kurosaka M, Matsui N, Yoshihara H, Tsunoda M, Mizuno K (2001) Histologic analysis of the implanted cartilage in an exact-fit osteochondral transplantation model. *Arthroscopy* 17:747-751
- Mankin HJ (1962) Localization of tritiated thymidine in articular cartilage of rabbits. II. Repair in immature cartilage. *J Bone Joint Surg Am* 44:688-698
- Mankin HJ (1982) The response of articular cartilage to mechanical injury. *J Bone Joint Surg Am* 64:460-466
- Matsusue Y, Yamamuro T, Hiromichi H (1993) Arthroscopic multiple osteochondral transplantation to the chondral defect in the knee associated with anterior cruciate ligament disruption. *Arthroscopy* 9:318-321
- Minas T, Nehrer S (1997) Current concepts in the treatment of articular cartilage defects. *Orthopedics* 20:525-538
- Nagai S, Asoh S, Kobayashi Y, Shidara Y, Mori T, Suzuki M, Moriyama Y, et al. (2007) Protection of hepatic cells from apoptosis induced by ischemia/reperfusion injury by protein therapeutics. *Hepato Res* 37:133-142
- Nakashima-Kamimura N, Nishimaki K, Mori T, Asoh S, Ohta S (2007) Prevention of chemotherapy-induced alopecia by the anti-death FNK protein. *Life Sci* 82:218-225
- Nam EK, Makhosous M, Koh J, Bowen M, Nuber G, Zhang LQ (2004) Biomechanical and histological evaluation of osteochondral transplantation in a rabbit model. *Am J Sports Med* 32:308-316
- Ohta Y, Kamiya T, Nagai M, Nagata T, Morimoto N, Miyazaki K, Murakami T, et al. (2008) Therapeutic benefits of intrathecal protein therapy in a mouse model of amyotrophic lateral sclerosis. *J Neurosci Res* 86:3028-3037
- Oshima Y, Watanabe N, Matsuda K, Takenaka N, Kawata M, Takai S (2002) Behavior of graft and host cells in underlying subchondral bone after transplantation of osteochondral autograft. *Microsc Res Tech* 58:19-24

- Outerbridge HK, Outerbridge AR, Outerbridge RE (1995) The use of a lateral patellar autologous graft for the repair of a large osteochondral defect in the knee. *J Bone Joint Surg Am* 77:65-72
- Ozaki D, Sudo K, Asoh S, Yamagata K, Ito H, Ohta S (2004) Transduction of anti-apoptotic proteins into chondrocytes in cartilage slice culture. *Biochem Biophys Res Commun* 313:522-527
- Patil S, Butcher W, D'Lima DD, Steklov N, Bugbee WD, Hoenecke HR (2008) Effect of osteochondral graft insertion forces on chondrocyte viability. *Am J Sports Med* 36:1726-1732
- Rosenberg L (1971) Chemical basis for the histological use of safranin-O in the study of articular cartilage. *J Bone Joint Surg Am* 53:69-82
- Sudo K, Asoh S, Ohsawa I, Ozaki D, Yamagata K, Ito H, Ohta S (2005) The anti-cell death FNK protein protects cells from death induced by freezing and thawing. *Biochem Biophys Res Commun* 330:850-856
- Tara S, Miyamoto M, Asoh S, Ishii N, Yasutake M, Takagi G, Takano T, et al. (2007) Transduction of the anti-apoptotic PTD-FNK protein improves the efficiency of transplantation of bone marrow mononuclear cells. *J Mol Cell Cardiol* 42:489-497
- Tew SR, Kwan AP, Hann A, Thomson BM, Archer CW (2000) The reactions of articular cartilage to experimental wounding: role of apoptosis. *Arthritis Rheum* 43:215-225
- Tibesku CO, Szuwart T, Kleffner TO, Schlegel PM, Jahn UR, Van Aken H, Fuchs S (2004) Hyaline cartilage degenerates after autologous osteochondral transplantation. *J Orthop Res* 22:1210-1214
- Whiteside RA, Jakob RP, Wyss UP, Mainil-Varlet P (2005) Impact loading of articular cartilage during transplantation of osteochondral autograft. *J Bone Joint Surg Br* 87:1285-1291
- Yamashita F, Sakakida K, Suzu F, Takai S (1985) The transplantation of an autogenic osteochondral fragment for osteochondritis dissecans of the knee. *Clin Orthop Relat Res* 201:43-50



Consumption of Molecular Hydrogen Prevents the Stress-Induced Impairments in Hippocampus-Dependent Learning Tasks during Chronic Physical Restraint in Mice

Kazufumi Nagata¹, Naomi Nakashima-Kamimura¹, Toshio Mikami², Ikuroh Ohsawa^{1,3} and Shigeo Ohta^{*1}

¹Department of Biochemistry and Cell Biology, Institute of Development and Aging Sciences, Graduate School of Medicine, Nippon Medical School, Kawasaki, Japan; ²Department of Health and Sports Science, Nippon Medical School, Kawasaki, Japan; ³Center of Molecular Hydrogen Medicine, Institute of Development and Aging Sciences, Nippon Medical School, Kawasaki, Japan

We have reported that hydrogen (H₂) acts as an efficient antioxidant by gaseous rapid diffusion. When water saturated with hydrogen (hydrogen water) was placed into the stomach of a rat, hydrogen was detected at several μM level in blood. Because hydrogen gas is unsuitable for continuous consumption, we investigated using mice whether drinking hydrogen water *ad libitum*, instead of inhaling hydrogen gas, prevents cognitive impairment by reducing oxidative stress. Chronic physical restraint stress to mice enhanced levels of oxidative stress markers, malondialdehyde and 4-hydroxy-2-nonenal, in the brain, and impaired learning and memory, as judged by three different methods: passive avoidance learning, object recognition task, and the Morris water maze. Consumption of hydrogen water *ad libitum* throughout the whole period suppressed the increase in the oxidative stress markers and prevented cognitive impairment, as judged by all three methods, whereas hydrogen water did not improve cognitive ability when no stress was provided. Neural proliferation in the dentate gyrus of the hippocampus was suppressed by restraint stress, as observed by 5-bromo-2'-deoxyuridine incorporation and Ki-67 immunostaining, proliferation markers. The consumption of hydrogen water ameliorated the reduced proliferation although the mechanistic link between the hydrogen-dependent changes in neurogenesis and cognitive impairments remains unclear. Thus, continuous consumption of hydrogen water reduces oxidative stress in the brain, and prevents the stress-induced decline in learning and memory caused by chronic physical restraint. Hydrogen water may be applicable for preventive use in cognitive or other neuronal disorders.

Neuropsychopharmacology (2009) 34, 501–508; doi:10.1038/npp.2008.95; published online 18 June 2008

Keywords: adult neurogenesis; cognition; hippocampus; molecular hydrogen; oxidative stress; preventive medicine

INTRODUCTION

Oxidative stress is widely accepted as a contributor to neuronal vulnerability (Langley and Ratan, 2004; Lin and Beal, 2006; Ohta and Ohsawa, 2006; Sayre *et al*, 2008). Thus, suitable antioxidants are desired to protect neural precursors and neurons against oxidative damage in the brain (Ferri *et al*, 2003); however, most antioxidants are not able to reach neurons because of the blood–brain barrier. We have recently reported that molecular hydrogen (H₂) reduces oxidative stress (Ohsawa *et al*, 2007; Fukuda *et al*, 2007), and can penetrate the blood–brain barrier to protect neurons by gaseous diffusion; however, inhalation of

hydrogen gas may be unsuitable as continuous hydrogen consumption for preventive use. A brief report has suggested that consumption of water containing hydrogen at a saturated level (hydrogen water) reduces oxidative stress in rats, as shown by decreased levels of urine oxidized guanine and hepatic lipid peroxide (Yanagihara *et al*, 2005). Thus, we examined the effect of hydrogen water on cognitive decline induced by oxidative stress.

Adult hippocampal neurogenesis may be involved in cognitive functions, including learning and memory, and spatial recognition (Abrous *et al*, 2005; Bruel-Jungerman *et al*, 2007). Antidepressants increase adult neurogenesis (Dranovsky and Hen, 2006; Becker and Wojtowicz, 2007; Sahay and Hen, 2007), suggesting that suppression of adult neurogenesis may be responsible for some mental disorders. Here we show that when chronic physical stress was applied to mice continuous consumption of hydrogen water reduced oxidative stress in the brain, and prevented the decline in the proliferation of progenitor neural cells and the impairment of cognitive function.

*Correspondence: Professor S Ohta, Department of Biochemistry and Cell Biology, Institute of Development and Aging Sciences, Graduate School of Medicine, Nippon Medical School, 1-396 Kosugi-cho, Nakahara-ku, Kawasaki 211-8533, Japan. Tel: +81 44 733 9267 Fax: +81 44 733 9268, E-mail: ohta@nms.ac.jp
Received 24 March 2008; revised 19 May 2008; accepted 23 May 2008

MATERIALS AND METHODS

Hydrogen Water

Molecular hydrogen (H₂) was dissolved in water under high pressure (0.4 MPa) to a supersaturated level using hydrogen water-producing apparatus (ver. 2) produced by Blue Mercury Inc. (Tokyo, Japan). The saturated hydrogen water (500 ml) was stored under atmospheric pressure in an aluminum bag with no dead volume. Hydrogen water was freshly prepared every week, which ensured that a concentration of more than 0.6 mM was maintained. We confirmed the hydrogen content with a hydrogen electrode (ABLE). Each day, hydrogen water from the aluminum bag was placed into a closed glass vessel (70 ml) equipped with an outlet line having two ball bearings, which kept the water from being degassed. This vessel ensured that the hydrogen concentration was more than 0.4 mM after 1 day. Hydrogen water degassed by gentle stirring was used for control animals; the complete removal of hydrogen gas was confirmed with the hydrogen electrode.

Measurement of Hydrogen in Blood

Hydrogen water (3.5 ml at 0.8 mM) was placed into the stomach of a rat (approximately 230 g) by a catheter. After 3 min, 5 ml of venous blood was collected from the heart and placed into a small aluminum bag containing 25 ml air. After hydrogen gas from blood was transferred into the air, 20 ml of the air from the aluminum bag was applied to gas chromatography to examine the content of hydrogen as described (Ohsawa et al, 2007).

Malondialdehyde Measurement

Brain malondialdehyde (MDA) levels were determined using a Bioxytech MDA-586 Assay Kit (OxisResearch, Oregon). Briefly, the frozen left brains were homogenized in the presence of butylated hydroxytoluene. After centrifugation, free MDA in the supernatant was converted to a stable carbocyanine dye (maximum absorption at 586 nm) by chemical reaction with *N*-methyl-2-phenylindole. MDA levels were normalized against protein concentration.

Physical Restraint Stress

This study was approved by the Animal Care and Use Committee of Nippon Medical School. We obtained ICR mice, 7 weeks of age (33–34 g body weight), from CLEA Japan Inc. (Tokyo, Japan), and divided 40 mice into four groups (each group had 10 mice) by the following combination. Stress and CTL: groups with and without restraint stress, respectively. HW(+) and HW(-): groups given water with and without hydrogen, respectively. Each mouse was placed in a 3 × 3 × 7.5 cm stainless-steel cage, which completely restricted their movement, but allowed them to drink water *ad libitum*. Immobilization stress was given 10 h per day (0900–1900 hours) for 6 days each week. Each immobilized mouse was housed individually in a small 10 × 10 × 10 cm compartment of a multicompartiment cage for the remaining time to avoid aggression and to prevent social isolation. Hydrogen water or degassed water was available *ad libitum* throughout the whole period. Unstressed

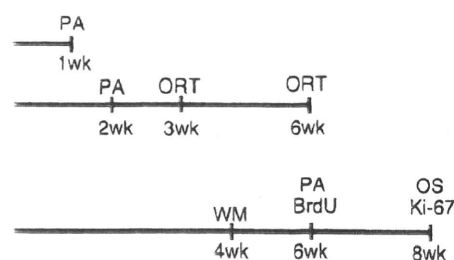


Figure 1 Schedules for subjecting mice to restraint stress and performing experiments are illustrated. Single bar indicates a series of experiments using the same mice. PA, ORT, WM, 5-bromo-2'-deoxyuridine (BrdU), Ki-67, and OS indicate the time points for passive avoidance, object recognition test, Morris water maze, injection of BrdU, and sampling for Ki-67 and oxidative stress (4-hydroxy-2-nonenal (HNE) staining and malondialdehyde (MDA) measurement). During the experiments of the Morris water maze, mice continued to be immobilized for 8 h per day.

mice were housed in standard-sized cages consisting five mice per cage, and they were handled daily without stress. Schedules for providing restraint stress and performing experiments are schematically illustrated in Figure 1.

Passive Avoidance Learning

The apparatus consisted of two compartments, one light and the other dark, separated by a vertical sliding door (O'Riordan et al, 2006). We initially placed a mouse in the light compartment for 20 s. After the door was opened, the mouse could enter the dark compartment (mice instinctively prefer being in the dark). After the mouse entered the dark compartment, the door was closed. After 20 s, the mouse was given a 0.3 mA electric shock for 2 s. The mouse was allowed to recover for 10 s, and was then returned to the home cage. After 24 h, the mouse was again placed in the light section with the door opened to allow the mouse to move into the dark section. We scored the latency time for stepping through the door. In addition, the number of mice that stayed in the light section for more than 300 s was recorded.

Object Recognition Task

The novel-object recognition and memory retention test was used to examine recognition memory (Wang et al, 2004; De Rosa et al, 2005). A mouse was habituated in a cage for 4 h, and then two different-shaped objects were presented to the mouse for 10 min as training. The number of times of explorations and/or sniffs of one object, which will be replaced with a novel one, was counted for the initial 5-min period (Training). To test memory retention after 1 day, one of the original objects was replaced with the novel one with a different shape, and then the number of times of explorations and/or sniffs of the novel one was counted for 5 min (Retention test). The recognition index was obtained as the frequencies (%) of exploring and/or sniffing the original object or the novel one.

Spatial Learning

Mice were trained on the Morris water maze (Morris et al, 1982; D'Hooge and De Deyn, 2001), with four trials per day

over 6 days. The water maze was a circular pool filled with water at room temperature (diameter, 125 cm; height, 55 cm; water temperature, $24 \pm 1^\circ\text{C}$). A transparent platform (diameter, 10 cm) was hidden 1 cm below the surface of water that had been made opaque with white nontoxic paint. Starting points were changed every day. Each trial lasted until either the mouse had found the platform or for a maximum of 60 s. The examiner determined the time of swimming until the mouse reached the platform (latency) using a stopwatch and a video. All mice were allowed to rest on the platform for 20 s. The platform was removed for a probe trial 24 h after the last training session on day 6. Retention of the spatial training was assessed 1 h after the last training trial. The single-probe trial consisted of a 60 s free swim in the pool without the platform. Mice were placed and released opposite the site where the platform had been located and the time spent in each quadrant was recorded for the probe trial. During the experiments, mice continued to be immobilized for 8 h per day, instead of 10 h.

Immunohistochemistry

After 8-week restraint stress, mice were perfused transcardially with saline under anesthesia. The right brain hemisphere and the cerebellum were removed and fixed in 4% paraformaldehyde in 0.1 M phosphate buffer (PB, pH 7.4) for 24 h at room temperature. Coronal sections (40 μm) were cut rostrocaudally with a vibratome (Leica, Cambridge, UK) and immersed in PBS.

For 5-bromo-2'-deoxyuridine (BrdU) immunohistochemistry, BrdU (Sigma) was dissolved in 0.9% NaCl and sterilized by filtration. After 6-week restraint stress, the mice received one intraperitoneal injection of 50 mg/kg body weight at a concentration of 10 $\mu\text{g}/\text{ml}$ per day for 5 consecutive days as described (Wolf *et al*, 2006). The sections were incubated in 2 N HCl at 37°C for 30 min to denature DNA, further incubated in 3% H₂O₂ in methanol for 30 min, and then blocked with mouse Ig blocking reagent from the M.O.M. kit (Vector Laboratories, Burlingame, CA) for 1 h. The primary antibody used was mouse monoclonal anti-BrdU (BD Pharmingen, 1:100).

For Ki-67 and 4-hydroxy-2-nonenal (HNE) immunoreactions, after 8-week restraint stress, sections were incubated in 10 mM citrate buffer (pH 6.0) at 90°C for 5 min, left to cool at room temperature, further incubated in 3% H₂O₂ in methanol for 30 min at 37°C , and then blocked with the M.O.M. kit and normal goat serum from the Vectastain ABC kit (Vector Laboratories), respectively. The primary antibodies used were rabbit polyclonal anti-Ki-67 antibody (Abcam, 1:500) and mouse monoclonal anti-HNE antibody (20 $\mu\text{g}/\text{ml}$; JaICA, Fukuroi, Japan). The HNE secondary antibody (M.O.M. biotinylated anti-mouse IgG, 1:250; Vector Laboratories) and the BrdU and Ki-67 secondary antibodies (biotinylated anti-rabbit IgG, 1:200) were applied for 2 h. The avidin/biotinylated mouse peroxidase complex (ABC kit; Vector Laboratories) was applied for 2 h, and the sections were stained with 3',3'-diaminobenzidine (Sigma) for 1 min.

Wire-Hanging Test

After 6-week restraint stress, neuromuscular strength was tested by wire-hanging test (Hamann *et al*, 2003). In brief,

mice were placed on wire netting, which was lightly shaken, causing the mouse to grip the wire. After the 20-s cutoff time, the wire netting was turned upside down (180°) and the time to falling was recorded.

Open-Field Test

After 7-week restraint stress, for the open-field test (Kim and Han, 2006), locomotor activity was measured in the open field of a white Plexiglas chamber ($36 \times 30 \times 18$ cm). Each mouse was individually placed in the left corner of an open field and locomotion was recorded for the indicated period. Horizontal locomotor activity was assessed according to the total rearing score for 20 min.

Statistical Analysis

All values are shown as the mean \pm standard error of measurement (SEM). Differences between groups were analyzed using one- or two-way ANOVA. When statistical differences were found, Fisher's PLSD *post hoc* test was performed. Statistical significance was accepted as $P < 0.05$. All the experiments were examined in a blinded fashion.

RESULTS

Physical Restraint Stress Enhanced Oxidative Stress and Hydrogen Water Decreased it

First, we examined whether hydrogen can be sufficiently incorporated into a body by drinking hydrogen water. Because it is difficult to obtain a sufficient volume of blood from mice, we used rats for the measurement of hydrogen concentration in the blood. We placed saturated hydrogen water at 3.5 ml per 230 g (15 ml/kg) directly into the stomach of a rat by a catheter. After 3 min, hydrogen was detected in the blood at the level of 5 μM (Figure 2a). Alternatively, an unpublished result suggests that the half-span of hydrogen in the muscle of rats is approximately 20 min as monitored with a needle-type hydrogen electrode, after the administration of hydrogen gas (data not shown).

We used mice for experiments of restraint stress. To examine whether mice preferably drank hydrogen water, we measured the volume of water consumed *ad libitum* by mice. The volume of water drunk by each mouse was nearly the same between groups drinking hydrogen water and degassed water (3.77 ± 0.11 vs 3.75 ± 0.08 ml, SEM).

Each mouse was then subjected to chronic physical restraint stress by placing it alone for 10 h per day in a very small cage, which completely restricted its movement, but allowed it to drink water *ad libitum*, and then was housed for 14 h in a small compartment as described in 'Materials and methods'. These treatments continued for 6 days per week. Water was available *ad libitum* throughout the whole period.

We examined the level of oxidative stress in the brain by immunohistologically estimating HNE, an end product of lipid peroxide (Ohsawa *et al*, 2003) after 8-week restraint stress (Figure 2b, c). Another oxidative marker, MDA, was estimated using a biochemical method (Fukuda *et al*, 2007; Figure 2d). These results revealed that chronic restraint stress enhanced oxidative stress in the brain. Notably, the

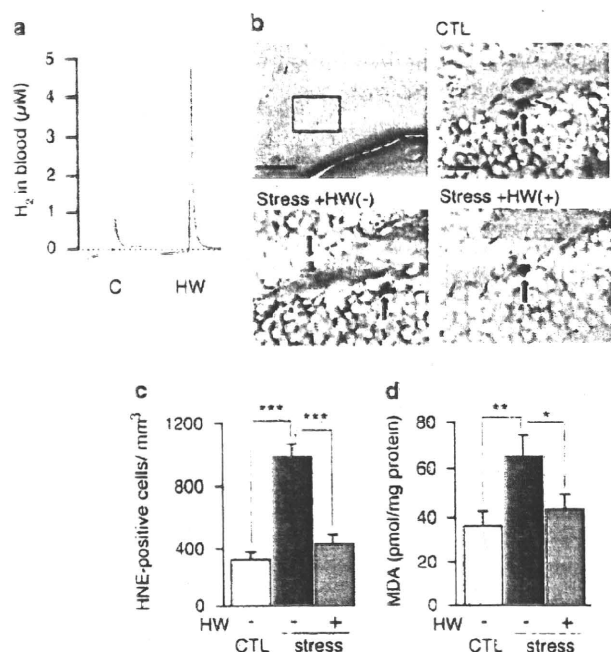


Figure 2 Consumption of hydrogen water reduced oxidative stress enhanced by restraint stress. (a) Hydrogen (H₂) in blood was measured 3 min after hydrogen water (3.5 ml) was placed directly into the stomach of a rat by a catheter. Profiles of gas chromatography are shown. (b) After 8-week exposure to restraint stress, the hippocampus region was stained with anti-4-hydroxy-2-nonenal (HNE)-conjugated peptide antibody. Representative photographs of HNE staining are shown. Arrows indicate positive cells. Scale bar: upper left panel, 100 μ m; magnified panels, 25 μ m. (c) HNE-positive cells in the dentate gyrus were counted using four serial sections ($F_{(2,27)} = 28.031$; $P < 0.0001$). (d) Malondialdehyde in the whole brain was biochemically measured ($F_{(2,27)} = 4.177$; $P = 0.0263$). CTL, unstressed control group; Stress, group exposed to restraint stress for 8 weeks; HW(+), group provided with hydrogen water; and HW(-), group provided with degassed water. Data are shown as the mean \pm SEM (each group consisted 10 mice). * $P < 0.05$, ** $P < 0.01$, and *** $P < 0.001$ vs Stress + HW(-).

consumption of hydrogen water suppressed the accumulation of the oxidative stress markers (Figure 2b–d).

Passive Avoidance Learning, Novel Recognition Test, and Morris Water Maze

We examined learning and memory ability using the passive avoidance test (O’Riordan et al, 2006). Mice instinctively prefer a dark compartment; however, if an electric shock is given in the dark compartment, the mice are normally reluctant to reenter it. At 1 or 2 weeks after restraint stress, the memory of the electric shock tended to be lost in mice provided with control degassed water (Figure 3a, b). On the other hand, mice that were provided with hydrogen water *ad libitum* showed a trend toward improved learning and memory (Figure 3a, b). Six-week restraint stress significantly impaired learning and memory in mice consuming no hydrogen water, whereas consuming hydrogen water *ad libitum* significantly ameliorated or prevented the cognitive impairment induced by restraint stress (Figure 3c, left panel). In particular, more mice (fourfold) stayed in the light section for more than 300 s than control group without

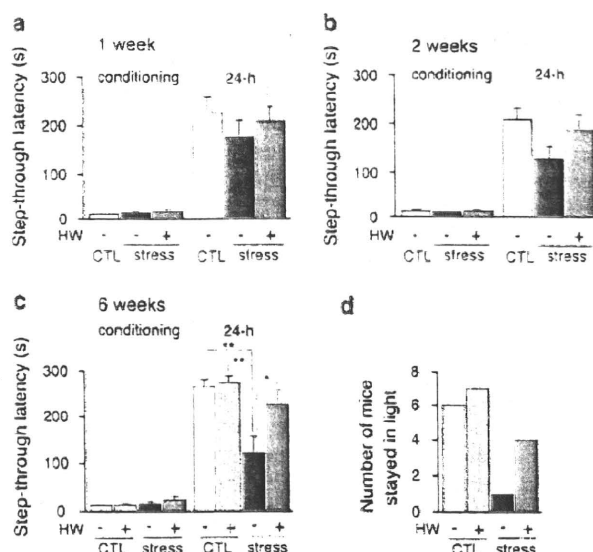


Figure 3 Passive avoidance test shows that hydrogen water prevented cognitive decline induced by restraint stress. After applying restraint stress for 1 week (a), 2 weeks (b), and 6 weeks (c) ($F_{(3,36)} = 7.661$; $P < 0.0005$), the passive avoidance test was performed by examining step-through latency time from light to dark compartments on the first day of the conditional trial (conditioning). At 24 h after an electric shock was given in the dark compartment, the latency time of mice moving from the light to dark compartment was measured (24 h). When a mouse did not enter the dark compartment for 300 s, the latency time was scored as 300 s. The number of mice that stayed in the light compartment for more than 300 s on the second day is shown (right panel). Stress and CTL groups with or without restraint stress, respectively; HW(+) and HW(-), groups given water with and without hydrogen, respectively. Experiments in (a), (b), and (c) were performed using different mice. * $P < 0.01$ and *** $P < 0.001$ vs Stress + HW(-). Data are the mean \pm SEM (each group consisted 10 mice).

hydrogen (Figure 3c, right panel). On the other hand, consumption of hydrogen water did not improve the cognitive ability when no stress was provided (Figure 3c).

As an alternative method to confirm impaired cognitive function after restraint stress, we applied the object recognition task (Wang et al, 2004; De Rosa et al, 2005; Ohsawa et al, 2008). If mice remember an object, they prefer to explore and/or sniff a novel object when the original object is replaced with the novel object. After 3-week restraint stress, hydrogen water tended to prevent or restore the decline in the recognition of a novel object, observed as a decreased frequency of exploring or sniffing the novel object (Figure 4a). The mice were subjected to the second object recognition task after 6-week stress, because the second test was available if the second objects were completely different from ones used in the first examination (Mouri et al, 2007). When restraint stress was applied for 6 weeks, consuming hydrogen water *ad libitum* significantly prevented or restored the decline in recognition and memory (Figure 4b). It should be noted that consumption of hydrogen water could not improve the cognitive ability when no stress was provided (Figure 4b).

To test spatial recognition and learning, we subjected mice to the Morris water maze (Morris et al, 1982; D’Hooge and De Deyn, 2001; Ohsawa et al, 2008). After 4-week restraint stress, the mice took longer to reach an invisible

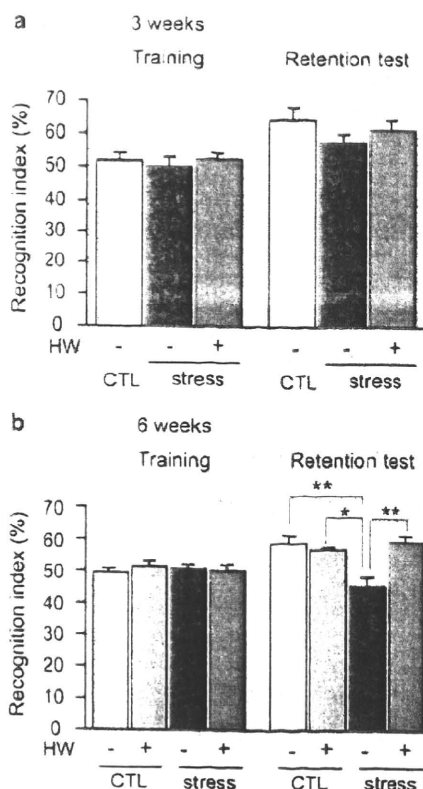


Figure 4 Object recognition task shows that hydrogen water prevented cognitive decline induced by restraint stress. For the object recognition task, after applying restraint stress for 3 (a) or 6 weeks (b) ($F_{(3,35)} = 7.466$; $P < 0.0005$), two different objects were presented to a mouse for 10 min for visual training and the number of times of explorations and/or sniffs of an object was counted in the initial 5-min period (Training). To test memory retention after 1 day, one of the original objects was replaced with the novel one with a different shape, and then the number of times of explorations and/or sniffs of the novel one was counted for 5 min (Retention test). The recognition indexes were obtained as the frequency (%) of exploring and/or sniffing the object that will be replaced, or the novel one that had been replaced. For example, if a mouse explored and/or sniffed only the novel object, the recognition index is scored as 100%, whereas if it did only the unchanged one, the recognition index is 0%. Stress and CTL groups with or without restraint stress, respectively; HW(+) and HW(-), groups given water with and without hydrogen, respectively. Experiments in (a) and (b) were performed using the same mice. When the second object recognition test was given to the same mice, objects that differed in shape and color were used. Data are the mean \pm SEM (each group consisted 10 mice). * $P < 0.01$ and ** $P < 0.001$ vs Stress + HW(-).

platform hidden in a pool after training than unstressed controls, indicating loss of memory of the platform location. Continuous consumption of hydrogen water shortened the time required for mice to reach the platform compared with stressed controls (Figure 5a). When the invisible platform is removed, mice should swim for longer near where the platform had previously been placed (the target quadrant) if they retain the memory of the platform location (Figure 5b, area A). Indeed, mice with chronic restraint stress swam around that location for a shorter time depending on their memory loss than unstressed controls (Figure 5c, area A). In contrast, stressed mice with consumption of hydrogen water swam in the target quadrant area (Figure 5b, area A) for a longer time than stressed controls without hydrogen

water, although no group showed significant difference in three nontarget quadrant areas (Figure 5c, areas B-D). Notably, hydrogen water consumption apparently improved spatial recognition and learning that had declined by restraint stress. This experiment also indicates that hydrogen water has no potential for improving the spatial cognitive ability when no stress was applied, which agrees with the previous results.

Hydrogen Water did not Affect Stress-Induced Reductions in Muscular Strength and Movement

To examine whether hydrogen water influenced the whole body, we monitored body weight during periods of restraint stress. Body weight decreased with restraint, and hydrogen water did not overcome this decrease (Supplementary Figure S1). Wire-hanging (Hamann *et al*, 2003) and open-field tests (Kim and Han, 2006) were used to exclude the possibility that hydrogen water influenced muscular strength and movement. Wire-hanging times depended on the body weight of each mouse, and no significant difference was observed in muscular strength (Supplementary Figure S2). Although restraint stress tended to affect movement, no effect of hydrogen water consumption was observed in the locomotion test (Supplementary Figure S3). Together, the behaviors observed by the three methods used to test cognitive function were not due to changes in movement ability, but indicated a decline in learning and memory. Thus, the improvement observed in the hydrogen water group was reflected by better learning ability and memory (Figures 3-5).

Hydrogen Water Improved the Proliferation of Progenitor Cells

Cognitive function may be involved in adult neurogenesis in the hippocampus. Finally, after 8-week restraint stress, we examined the correlation between adult neurogenesis and the hippocampal function by counting proliferating progenitor cells in the dentate gyrus of the hippocampus with BrdU labeling (Kee *et al*, 2002; Ekdahl *et al*, 2003). Positive nuclei, as judged by the shape and size, were counted in the boundary region of the dentate gyrus in four serial sections. Restraint stress decreased the number of proliferating cells, and hydrogen water significantly restored them (Figure 6a, b). As an alternative method, Ki-67 was used as a marker of proliferating cells (Kee *et al*, 2002; Shidara *et al*, 2005). The results were similar to those obtained by the BrdU-labeling method (Figure 6c, d). These findings suggest that continuous consumption of hydrogen water improves the proliferation of neural progenitor cells or adult neurogenesis impaired by restraint stress.

DISCUSSION

In summary, the continuous consumption of hydrogen water throughout the whole period of physical restraint stress reduced oxidative stress, prevented the decline in the proliferation of neural progenitors, and prevented cognitive decline, all of which are induced by chronic physical restraint stress. The restraint stress applied in this study may also induce considerable psychological as well as

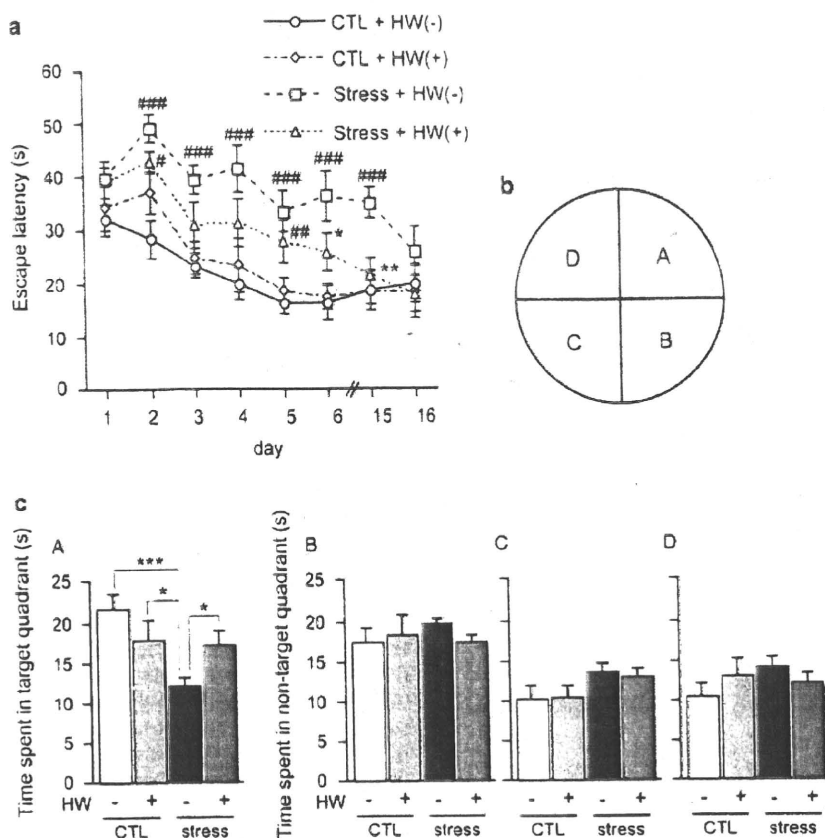


Figure 5 The Morris water maze shows that hydrogen water prevented cognitive decline induced by restraint stress. After applying restraint stress for 4 weeks, the time to reach a hidden platform was measured after four daily trials (a). During the experiments, mice continued to be immobilized for 8 h per day. (b) A single-probe trial consisted of a 60 s free swim in the pool without the platform. Quadrant areas used for the probe trial are shown, where the platform had been located in area A and mice were placed and released in region B. (c) At 6 days after daily training, after removing the platform, the time of free swimming in each area (A–D). Two parameters (stress and hydrogen) were analyzed by two-way ANOVA. Area A: $F_{(1,36)} = 4.455$; $P = 0.042$, area B: $F_{(1,36)} = 0.016$; $P = 0.901$, area C: $F_{(1,36)} = 0.933$; $P = 0.341$, and area D: $F_{(1,36)} = 3.235$; $P = 0.08$ by two-way ANOVA. Four groups were compared in area A by one-way ANOVA ($F_{(3,36)} = 5.074$; $P = 0.0049$). Stress and CTL, groups with or without restraint stress, respectively; HW(+) and HW(-), groups given water with and without hydrogen, respectively. Data are the mean \pm SEM (each group consisted 10 mice). * $P < 0.05$, ** $P < 0.01$, and *** $P < 0.001$ vs Stress + HW(-). # $P < 0.05$, ## $P < 0.03$ vs CTL + HW(-); ### $P < 0.01$ vs CTL + HW(-) and CTL + HW(+).

physical stress. In this study, we examined impaired learning and memory by three different methods: passive avoidance learning, object recognition task, and the Morris water maze. In these methods, successive object recognition tasks are available (Mouri *et al*, 2007) and the Morris water maze gives no influence on results of passive avoidance test (Yamada *et al*, 1999; King and Arendash, 2002). Thus, some experiments were performed using the same mice as shown in Figure 1, although a possibility cannot be ruled out that the passive avoidance test was influenced by the water-maze training.

We have recently reported that hydrogen reduced hydroxyl radicals, the most reactive oxygen species (ROS), and protected cells against oxidative stress. Inhalation of 1% hydrogen gas was enough to protect the brain and liver (Ohsawa *et al*, 2007; Fukuda *et al*, 2007), where the hydrogen in blood should be 8 μ M because the saturated level of hydrogen reached 800 μ M under atmospheric pressure. It is possible that continuous consumption of hydrogen defends the brain against chronic oxidative stress even at much lower concentrations than 8 μ M. In this study,

we showed that the incorporation of hydrogen from the stomach into blood reached 5 μ M. Continuous exposure to hydrogen may change blood components toward the reductive state, and indirectly influence the oxidative state in the brain. Although it remains unclear how hydrogen reduces oxidative stress in the brain, the present study may highlight the prominent role of oxidative stress in deficits of learning and memory.

The consumption of hydrogen water ameliorated the proliferation of neural progenitors that had been declined by restraint stress although the mechanistic link between the changes in neurogenesis and cognitive impairments is at this stage correlative. However, adult neurogenesis may be involved in hippocampal functioning, including learning and memory and spatial recognition processes, and affected by multiple intrinsic and extrinsic factors. For example, adult neurogenesis is suppressed by cranial radiotherapy, stress-sensitive adrenal hormones such as glucocorticoids, and physical or psychological stress, and improved with inflammatory blockade. When we studied oxidative stress, we found growing evidence suggesting that it is involved

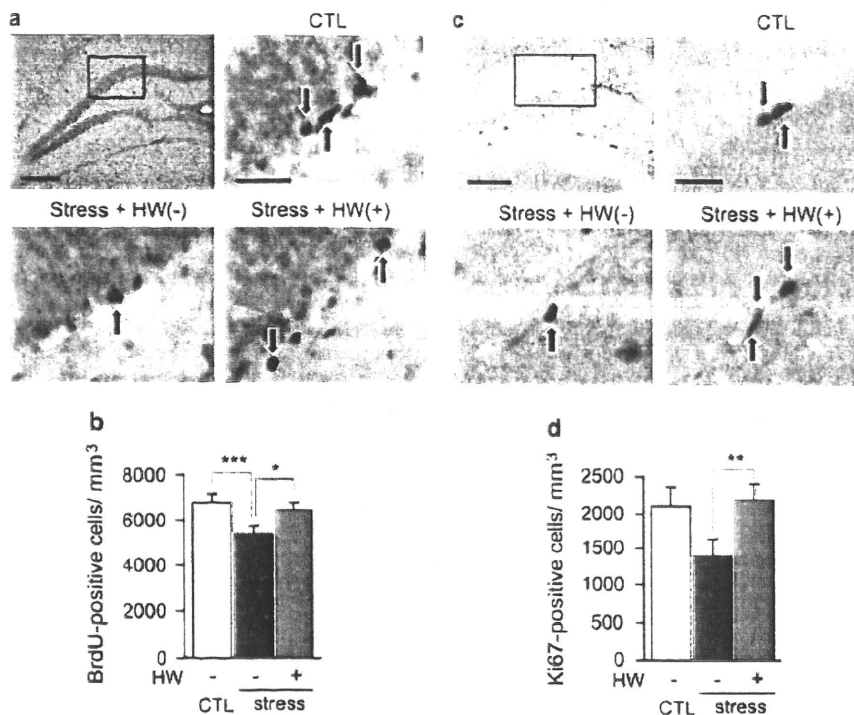


Figure 6 Hydrogen restores the proliferation of progenitor cells declined by restraint stress. (a) Mice were injected with 5-bromo-2'-deoxyuridine (BrdU) after 6-week restraint stress. Representative photographs of BrdU-positive progenitor cells in the dentate gyrus of the hippocampus are shown. Arrows indicate positive cells. Scale bar: upper left panel, 100 μ m; magnified panels, 25 μ m. (b) BrdU-positive nuclei of progenitor cells in the boundary region of the dentate gyrus of the hippocampus were counted in four serial sections ($F_{(2,27)} = 4.289$; $P = 0.0241$). (c) Cell proliferation in the dentate gyrus was examined using anti-Ki-67 antibody. Representative photographs of Ki-67-positive cells in the dentate gyrus of the hippocampus are shown. Arrows indicate positive cells. Scale bar: upper left panel, 100 μ m; magnified panels, 25 μ m. (d) Ki-67-positive progenitor cells in the boundary region of the dentate gyrus were counted in four serial sections ($F_{(2,27)} = 3.155$; $P = 0.0587$). CTL, unstressed control group; Stress, group exposed to restraint stress for 8 weeks; HW(+), group provided with hydrogen water; and HW(-), group provided with degassed water. Data are the mean \pm SEM (each group consisted 10 mice). * $P < 0.05$, ** $P < 0.03$, and *** $P < 0.01$ vs Stress + HW(-).

downstream of contributors that affect adult neurogenesis: (1) radiotherapy produces hydroxyl radicals of ROS (Madsen *et al*, 2003; Raber *et al*, 2004), (2) an inflammatory blockade restores adult hippocampal neurogenesis, which may be elucidated by decreasing inflammatory oxidative stress (Ekdahl *et al*, 2003; Monje *et al*, 2003), (3) glucocorticoids enhance oxidative stress-induced cell death in the hippocampus (Behl *et al*, 1997), and (4) the present study and others have shown that restraint stress itself enhances oxidative stress in the brain (Liu *et al*, 1996; Kim *et al*, 2005; Luo *et al*, 2005).

Thus, it is possible that during the exposure to physical restraint stress continuous consumption of hydrogen water reduced oxidative stress in the brain, resulting in the improvement of adult neurogenesis or the stimulation of neural proliferation, leading to the prevention of the decline in learning and memory. This is the first report showing a benefit of drinking hydrogen water. Thus, we propose that hydrogen water is applicable as preventive treatment by reducing oxidative stress.

ACKNOWLEDGEMENTS

This study was supported by grants from the Japanese Ministries of Health, Labour, and Welfare (H-18-Choju-009,

Longevity Science) and Education, Culture, Sports, Science and Technology (19659331).

DISCLOSURE/CONFLICT OF INTEREST

Dr Ohta is a director of Mitos Co. Ltd (Kawasaki, Japan), and a scientific adviser to Blue Mercury Inc. (Tokyo, Japan). Blue Mercury Inc. supplied the fresh hydrogen water used in this study and has donated a research division to our institute. Other authors have no conflict of interest.

REFERENCES

- Abrous DN, Koehl M, Le Moal M (2005). Adult neurogenesis: from precursors to network and physiology. *Physiol Rev* 85: 523-569.
- Becker S, Wojtowicz JM (2007). A model of hippocampal neurogenesis in memory and mood disorders. *Trends Cogn Sci* 11: 70-76.
- Behl C, Lezoualc'h F, Trapp T, Widmann M, Skutella T, Holsboer F (1997). Glucocorticoids enhance oxidative stress-induced cell death in hippocampal neurons *in vitro*. *Endocrinology* 138: 101-106.
- Bruel-Jungerman E, Rampon C, Laroche S (2007). Adult hippocampal neurogenesis, synaptic plasticity and memory: facts and hypotheses. *Rev Neurosci* 18: 93-114.

- D'Hooge R, De Deyn PP (2001). Applications of the Morris water maze in the study of learning and memory. *Brain Res Rev* 36: 60–90.
- De Rosa R, Garcia AA, Braschi C, Capsoni S, Maffei L, Berardi N *et al* (2005). Intranasal administration of nerve growth factor (NGF) rescues recognition memory deficits in AD11 anti-NGF transgenic mice. *Proc Natl Acad Sci USA* 102: 3811–3816.
- Dranovsky A, Hen R (2006). Hippocampal neurogenesis: regulation by stress and antidepressants. *Biol Psychiatry* 59: 1136–1143.
- Ekdahl CT, Claassen JH, Bonde S, Kokaia Z, Lindvall O (2003). Inflammation is detrimental for neurogenesis in adult brain. *Proc Natl Acad Sci USA* 100: 13632–13637.
- Ferri P, Cecchini T, Ciaroni S, Ambrogini P, Cuppini R, Santi S *et al* (2003). Vitamin E affects cell death in adult rat dentate gyrus. *J Neurocytol* 32: 1155–1164.
- Fukuda K, Asoh S, Ishikawa M, Yamamoto Y, Ohsawa I, Ohta S (2007). Inhalation of hydrogen gas suppresses hepatic injury caused by ischemia/reperfusion through reducing oxidative stress. *Biochem Biophys Res Commun* 28: 670–674.
- Hamann M, Meisler MH, Richter A (2003). Motor disturbances in mice with deficiency of the sodium channel gene *Scn8a* show features of human dystonia. *Exp Neurol* 184: 830–838.
- Kee N, Sivalingam S, Boonstra R, Wojtowicz JM (2002). The utility of Ki-67 and BrdU as proliferative makers of adult neurogenesis. *J Neurosci Methods* 30: 97–105.
- Kim KS, Han PL (2006). Optimization of chronic stress paradigms using anxiety- and depression-like behavioral parameters. *J Neurosci Res* 83: 497–507.
- Kim ST, Choi JH, Chang JW, Kim SW, Hwang O (2005). Immobilization stress causes increases in tetrahydrobiopterin, dopamine, and neuromelanin and oxidative damage in the nigrostriatal system. *J Neurochem* 95: 89–98.
- King DL, Arendash GW (2002). Behavioral characterization of the Tg2576 transgenic model of Alzheimer's disease through 19 months. *Physiol Behav* 75: 627–642.
- Langley B, Ratan RR (2004). Oxidative stress-induced death in the nervous system: cell cycle dependent or independent? *J Neurosci Res* 77: 621–629.
- Lin MT, Beal MF (2006). Mitochondrial dysfunction and oxidative stress in neurodegenerative diseases. *Nature* 443: 787–795.
- Liu J, Wang X, Shigenaga MK, Yeo HC, Mori A, Ames BN (1996). Immobilization stress causes oxidative damage to lipid, protein, and DNA in the brain of rats. *FASEB J* 10: 1532–1538.
- Luo C, Xu H, Li XM (2005). Quetiapine reverses the suppression of hippocampal neurogenesis caused by repeated restraint stress. *Brain Res* 1063: 32–39.
- Madsen TM, Kristjansen PE, Bolwing TG, Wortwein G (2003). Arrested neuronal proliferation and impaired hippocampal function following fractionated brain irradiation in the adult rat. *Neuroscience* 119: 635–642.
- Monje ML, Toda H, Palmer TD (2003). Inflammatory blockade restores adult hippocampal neurogenesis. *Science* 302: 1760–1765.
- Morris RG, Garrud P, Rawlins JN, O'Keefe J (1982). Place navigation impaired rats with hippocampal lesions. *Nature* 297: 681–683.
- Mouri A, Noda Y, Hara H, Mizoguchi H, Tabira T, Nabeshima T (2007). Oral vaccination with a viral vector containing Abeta cDNA attenuates age-related Abeta accumulation and memory deficits without causing inflammation in a mouse Alzheimer model. *FASEB J* 21: 2135–2148.
- Ohsawa I, Ishikawa M, Takahashi K, Watanabe M, Nishimaki K, Yamagata K *et al* (2007). Hydrogen acts as a therapeutic antioxidant by selectively reducing cytotoxic oxygen radicals. *Nat Med* 13: 688–694.
- Ohsawa I, Nishimaki K, Murakami Y, Suzuki Y, Ishikawa M, Ohta S (2008). Age-dependent neurodegeneration accompanying memory loss in transgenic mice defective in mitochondrial ALDH2 activity. *J Neurosci* 28: 6239–6249.
- Ohsawa I, Nishimaki K, Yasuda C, Kamino K, Ohta S (2003). Deficiency in a mitochondrial aldehyde dehydrogenase increases vulnerability to oxidative stress in PC12 cells. *J Neurochem* 84: 1110–1117.
- Ohta S, Ohsawa I (2006). Dysfunction of mitochondria and oxidative stress in the pathogenesis of Alzheimer's disease: on defects in the cytochrome *c* oxidase complex and aldehyde detoxification. *J Alzheimers Dis* 9: 155–166.
- O'Riordan KJ, Huang IC, Pizzi M, Spano P, Boroni F, Egli R *et al* (2006). Regulation of nuclear factor kappaB in the hippocampus by group I metabotropic glutamate receptors. *J Neurosci* 26: 4870–4879.
- Raber J, Rola R, LeFevour A, Morhardt D, Curley J, Mizumatsu S *et al* (2004). Radiation-induced cognitive impairments are associated with change in indicators of hippocampal neurogenesis. *Radiat Res* 162: 39–47.
- Sahay A, Hen R (2007). Adult hippocampal neurogenesis in depression. *Nat Neurosci* 10: 1110–1115.
- Sayre LM, Perry G, Smith MA (2008). Oxidative stress and neurotoxicity. *Chem Res Toxicol* 21: 172–188.
- Shidara Y, Yamagata K, Kanamori T, Nakano K, Kwong JQ, Manfredi G *et al* (2005). Positive contribution of pathogenic mutations in the mitochondrial genome to the promotion of cancer by prevention from apoptosis. *Cancer Res* 65: 1655–1663.
- Yamada K, Tanaka T, Han D, Senzaki K, Kameyama T, Nabeshima T (1999). Protective effects of idebenone and alpha-tocopherol on beta-amyloid-(1-42)-induced learning and memory deficits in rats: implication of oxidative stress in beta-amyloid-induced neurotoxicity *in vivo*. *Eur J Neurosci* 11: 83–90.
- Yanagihara T, Arai K, Miyamae K, Sato B, Shudo T, Yamada M *et al* (2005). Electrolyzed hydrogen saturated water for drinking use elicits an antioxidative effect: a feeding test with rats. *Biosci Biotechnol Biochem* 69: 1985–1987.
- Wang H, Ferguson GD, Pineda VV, Cundiff PE, Storm DR (2004). Overexpression of type-1 adenylyl cyclase in mouse forebrain enhances recognition memory and LTP. *Nat Neurosci* 7: 635–642.
- Wolf SA, Kronenberg G, Lehmann K, Blankenship A, Overall R, Staufenbiel M *et al* (2006). Cognitive and physical activity differently modulate disease progression in the amyloid precursor protein (APP)-23 model of Alzheimer's disease. *Biol Psychiatry* 60: 1314–1323.

Supplementary Information accompanies the paper on the Neuropsychopharmacology website (<http://www.nature.com/npp>)

Brief communication

Cytoprotective role of mitochondrial amyloid β peptide-binding alcohol dehydrogenase against a cytotoxic aldehyde

Yayoi Murakami^{a,b}, Ikuroh Ohsawa^a, Tadashi Kasahara^b, Shigeo Ohta^{a,*}

^a Department of Biochemistry and Cell Biology, Institute of Development and Aging Sciences, Graduate School of Medicine, Nippon Medical School, 1-396 Kosugi-cho, Nakahara-ku, Kawasaki-city, Kanagawa-pref. 211-8533, Japan

^b Department of Biochemistry, Kyoritsu University of Pharmacy, Japan

Received 15 January 2007; received in revised form 30 May 2007; accepted 9 July 2007

Available online 20 August 2007

Abstract

Recent reports on amyloid β peptide (A β) binding-alcohol dehydrogenase (ABAD) have revealed the link of A β with oxidative stress derived from mitochondria in the pathogenesis of Alzheimer's disease (AD). As a novel function of ABAD, we speculate that ABAD may detoxify aldehydes, such as 4-hydroxy-2-nonenal (4-HNE). To verify this speculation, we transfected cDNA encoding ABAD into cultured cells (HeLa and SH-SY5Y), where ABAD was localized to mitochondria. ABAD-transfectants decreased the levels of externally added 4-HNE in cultured medium as detected by TLC and became resistant against external 4-HNE. Moreover, ABAD suppressed the cytotoxic effects caused by cellular 4-HNE, which were produced through excess reactive oxygen species (ROS) by treatment with an inhibitor of mitochondrial respiration, antimycin A or by adding H₂O₂. Catabolism of 4-HNE by ABAD was inhibited by A β , resulting in the abolishment of the cytoprotective function by ABAD against ROS. These results propose an additional role of ABAD in neural cell death in AD: ABAD detoxifies aldehydes, such as 4-HNE derived from lipid peroxides in healthy brains, and inhibited by A β in the development of AD. © 2007 Elsevier Inc. All rights reserved.

Keywords: ADH; Alzheimer's disease; A β ; 4-Hydroxy-2-nonenal; HNE; Lipid peroxide; Mitochondria; Oxidative stress

1. Introduction

Accumulation of amyloid β peptide (A β) has been widely accepted as a central event for the development of Alzheimer's disease (AD) (Selkoe, 1994). On the other hand, many reports support the contribution of the decrease in energy production and the increase in oxidative stress, both of which are due to mitochondrial dysfunction (Ohsawa et al., 2003; Ohta, 2003); however, the relationship between mitochondrial dysfunction and A β has remained unclear for a long time. Recently, it has been revealed that some A β localizes to mitochondria (Manzaki et al., 2006). In particular, reports on the binding of A β to mitochondrial A β -binding alcohol dehydrogenase (ABAD) highlighted the molecular link of A β with the role of mitochondria. A β interacts with ABAD with

high specificity and inhibits its enzymatic activity, leading to the generation of reactive oxygen species (ROS) (Lustbader et al., 2004).

4-Hydroxy-2-nonenal (4-HNE) is widely used as a marker of excess oxidative stress, because it is a non-enzymatic end-product derived from lipid peroxides (LPO) (Mark et al., 1997). 4-HNE is highly toxic by readily binding with lysine, histidine, serine, and cysteine residues (Uchida and Stadtman, 1992). The accumulation of LPO and 4-HNE has been reported in neurodegenerative disorders including AD (Sayre et al., 1997). We have previously proposed that ALDH2 is involved in the detoxification of 4-HNE generated by oxidative stress of mitochondria and that defects in ALDH2 activity cause neuronal death by stimulating the accumulation of 4-HNE due to oxidative stress (Ohsawa et al., 2003).

Alcohols [–CH₂OH] are reversibly converted into aldehydes [–CH=O] by alcohol dehydrogenases in the presence of

* Corresponding author. Tel.: +81 44 733 9267; fax: +81 44 733 9268.
E-mail address: ohta@nms.ac.jp (S. Ohta).

NAD⁺, while aldehydes are irreversibly converted into acids [–C(–OH)=O] by aldehyde dehydrogenases in the presence of NAD⁺ (Suzuki et al., 2004). Thus, we speculate that ABAD may function as a detoxifier of cytotoxic aldehydes and that A β may disturb the function leading to the accumulation of aldehydes that accelerate neuronal death. In this study, we tried to verify the working hypothesis. Here we show that A β inhibits the activity of ABAD to catabolize 4-HNE and abolishes the cytoprotective role of ABAD.

2. Materials and methods

2.1. Plasmid construction, cell culture and transfection

Cloned full-length human cDNA encoding ABAD (named *HADH2*) was composed of the cytomegalovirus (CMV) immediate early promoter, SV40 early mRNA polyadenylation signal, and a neomycin resistance cassette. Nucleotide sequence of ABAD cDNA was confirmed by direct sequencing. HeLa and SH-SY5Y neuroblastoma cells were transfected with ABAD cDNA after digestion of *Apa* I for linearization, cloned using 400 and 600 μ g/mL of Geneticin[®] (Gibco BRL Invitrogen, Stockholm, Sweden), respectively. HeLa and SH-SY5Y transfectants were placed at a density of 2×10^4 and 5×10^4 cells/cm², respectively, for experiments throughout this study.

2.2. Detection of 4-HNE catabolism and accumulation

The HeLa transfectants were placed on a 9 cm dish and the medium was exchanged with 1 mL of Krebs–Henseleit buffer containing 250 μ M 4-HNE and incubated at 37 °C for 15 or 30 min. TLC was used to semi-quantify 4-HNE with a modified previous method (Burczynski et al., 2001) by using pure 4-HNE (Calbiochem, San Diego, CA, USA) as a standard. Intensities of TLC spots with R_f = 0.49 were quantified with NIH image software to calculate the amount of 4-HNE remaining in the supernatant. When A β pretreatment is necessary, the A β peptide (A β _{1–42} (human), Biosource, Camarillo, CA, USA) was incubated for 4 days at 37 °C to be aggregated in PBS and added to cell culture to 1 μ g/mL in DMEM/F12 containing 1% FBS for 14 h at 37 °C.

We placed HeLa transfectants on 4-well plastic plates (SonicSeal slide; Nalge Nunc, Rochester, NY, USA) and imaged proteins conjugated with 4-HNE by using anti-4-HNE antibody as described previously (Ohsawa et al., 2003). Pixel intensity was measured with NIH image.

2.3. Treatments with 4-HNE, antimycin A or H₂O₂

To examine cell viability, cells were placed in 96-well plates and treated with 4-HNE, H₂O₂ or antimycin A in DMEM/F-12 medium containing 1% FBS for 24 h, followed by staining with 10 μ M propidium iodide (PI; to detect nuclei of dead cells) and 10 μ M Hoechst 33342 (for nuclei of total

cells). The cells stained were with PI and/or Hoechst under a fluorescence microscope to calculate the percentage of dead cells. When necessary, pretreatment with aggregated A β was performed as above.

2.4. Statistical analysis

Statistical analyses were performed using StatView software (SAS Institute). Unpaired two-tailed Student *t*-test and ANOVA followed by Fisher's exact test were used for single and multiple comparisons, respectively. Experiments for quantification were performed in a blinded fashion.

3. Results

3.1. ABAD catabolizes 4-HNE to protect cells

To reveal the role of ABAD in living cells, we transfected *HADH2* cDNA into HeLa cells or SH-SY5Y neuroblastomas to overexpress ABAD and confirmed its overexpression by Western blotting (Supplementary-Fig. 1). Two clones from each transfectant were used for this study; ABAD-positive clones are A1, A2 (HeLa) and A3, A4 (SH-SY5Y); and vector control transfectants are V1, V2 (HeLa) and V3, V4 (SH-SY5Y). Then, we imaged ABAD with its specific antibody by confocal laser scanning microscopy: the majority of ABAD localized to mitochondria (Supplementary-Fig. 2), which is in good agreement with previous reports (Lustbader et al., 2004; Yang et al., 2005).

First, we examined whether ABAD-transfectants catabolize 4-HNE by TLC. Thirty minutes after exposure to 4-HNE (250 μ M), we found significant decrease in the levels of 4-HNE in the media in ABAD-transfectants more than controls at 30 min (Fig. 1A and Supplementary-Fig. 3A). Since 4-HNE rapidly modifies proteins, the possibility is not ruled out that the decrease in 4-HNE in the media may be due to only the acceleration of incorporation of 4-HNE. As 4-HNE is produced from lipid peroxides in a non-enzymatic manner, we forced to generate superoxide radicals by treatment with a mitochondrial respiratory inhibitor, antimycin A (Schulze-Osthoff et al., 1992), and then detected proteins conjugated with 4-HNE by immunostaining using its specific antibody. The amount of proteins conjugated with 4-HNE in ABAD-negative transfectants significantly increased more than ABAD-transfectants after treatment with 15 μ g/mL antimycin A (Fig. 1B and Supplementary-Fig. 3B); therefore, it is concluded that ABAD catabolizes 4-HNE.

Next, we examined the cytoprotective effects of ABAD against 4-HNE. Considerable dead cells after treatment with 10 μ M 4-HNE for 24 h were found in control transfectants in a dose-dependent manner, whereas fewer dead cells were seen in ABAD-transfectants (Fig. 1C and Supplementary-Fig. 4A). Moreover, we examined the cytoprotective role of ABAD against 4-HNE in neuroblastomas. Twenty-four hour after co-transfection of SH-SY5Y cells with the ABAD and

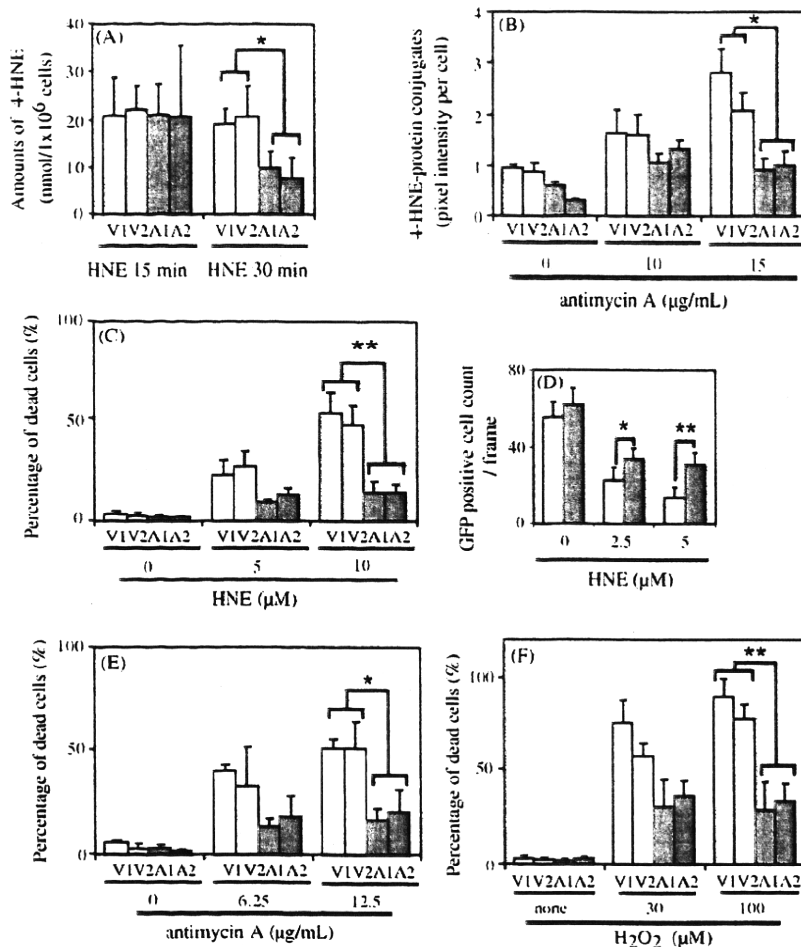


Fig. 1. ABAD catabolizes *exogenous* and *endogenous* 4-HNE. (A) Each HeLa transfectant was treated with external 4-HNE (250 μM). The external 4-HNE was extracted from the supernatant medium, spotted onto TLC and quantified (see Supplementary-Fig. 3A). (B) 4-HNE-protein conjugates in each HeLa transfectant after treatment with antimycin A were quantified from pixel intensity in cells stained with anti-4-HNE antibody (see Supplementary-Fig. 3B). (C) Percentage of dead cells of each HeLa transfectant after treatment with 4-HNE for 24 h (see Supplementary-Fig. 4A). (D) SH-SY5Y cells were transiently co-transfected with EGFP/vector or EGFP/ABAD, and then treated with 4-HNE for 24 h, and living cells expressing EGFP were enumerated under a fluorescent microscope. Open and grey bars indicate co-transfectants of EGFP with empty vector and the ABAD cDNA, respectively (see Supplementary-Fig. 4B). ***p* < 0.01 in Student's *t*-test. Note that transfection efficiency was approximately 70% as judged by the appearance of EGFP-positive cells without 4-HNE. (E) Percentage of dead cells of each stable HeLa transfectant after treatment for 24 h with antimycin A (see Supplementary-Fig. 4C). Note that antimycin A induces superoxides that may accelerate lipid-peroxidation and accumulate 4-HNE. (F) Percentage of dead cells of each stable HeLa transfectant after treatment for 24 h with H₂O₂ (see Supplementary-Fig. 4D). Note that H₂O₂ accelerates lipid-peroxidation and accumulates 4-HNE. (A–F) A1, A2: ABAD-expressing HeLa; and A3, A4: ABAD-expressing SH-SY5Y; V1, V2: vector control HeLa transfectants, and V3, V4: vector control SH-SY5Y transfectants. Data are the mean ± S.D. (*n* = 4). **p* < 0.05; ***p* < 0.01 in ANOVA (A–F) or Student's *t*-test (D).

EGFP genes, treatment with 4-HNE for 24 h decreased the EGFP-positive cells due to cell death; however, vector/EGFP co-transfectants were less than ABAD/EGFP, indicating ABAD-transfectants were more resistant against the 4-HNE-treatment (Fig. 1D and Supplementary-Fig. 4B). Thus, these experiments suggest that ABAD catabolizes 4-HNE to protect cells.

The protective ability against cell death was examined by treatment with antimycin A and hydrogen peroxide (H₂O₂). Considerable dead cells in controls were seen after treatment, whereas ABAD-transfectants were resistant to the treatment

(Fig. 1E and F, Supplementary-Fig. 4C and D). Therefore, ABAD makes cells cytoprotective against oxidative stress.

3.2. Cytoprotective role of ABAD is suppressed by Aβ

When cell cultures are exposed to Aβ, Aβ binds to ABAD (Yan et al., 1997). Thus, we examined whether Aβ actually inhibits ABAD activity in the detoxification of 4-HNE. When HeLa transfectants were treated with Aβ_{1–42}, it inhibited the decrease in external 4-HNE only in ABAD-transfectants (Fig. 2A). Moreover, Aβ_{1–42} inhibited the cytoprotective role

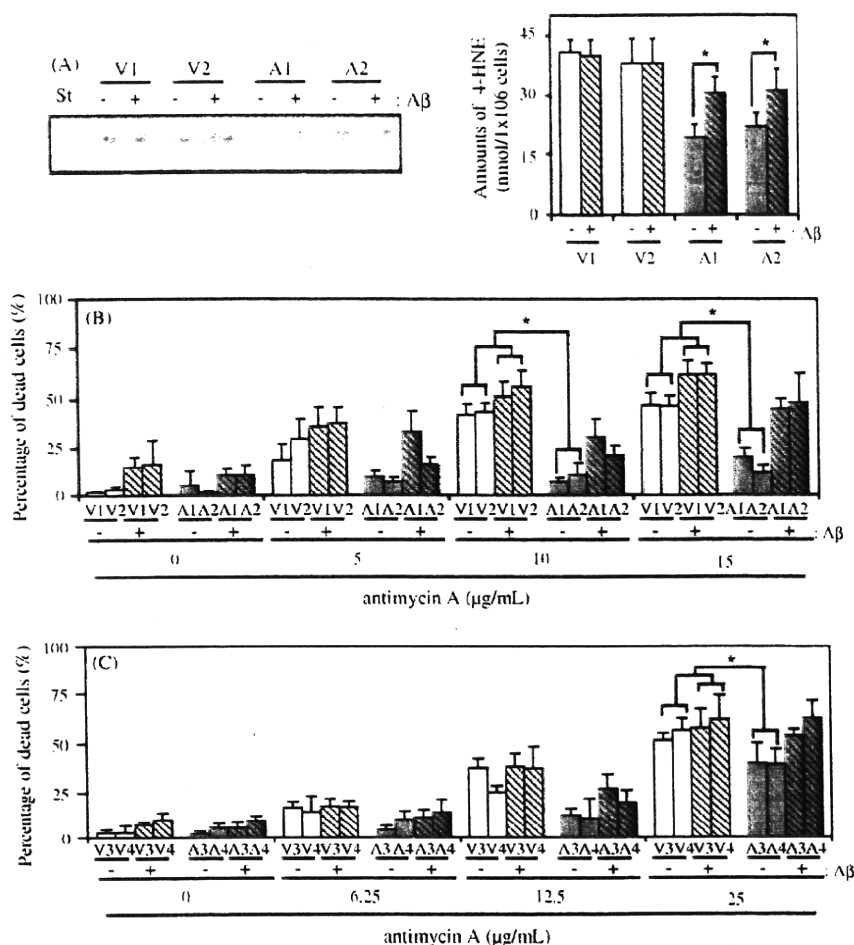


Fig. 2. Inhibition of the ABAD activity by A β . (A) Each transfectant was pretreated with A β (1 μ g/mL) for 14 h, and then with external 4-HNE (250 μ M) for 30 min. (Left) Representative patterns of TLC for quantifying residual 4-HNE in medium are shown. (Right) Amounts of residual 4-HNE were quantified. (B and C) Each transfectant of HeLa (B) and SH-SY5Y (C) was pretreatment with A β for 14 h, and then with antimycin A for 24 h, and stained with Hoechst33342 (blue: dead and living cells) and PI (pink: dead cells) to obtain percentage of dead cells. (A–C) A β + and – indicate with and without preincubation with A β . A1, A2: ABAD-expressing HeLa, and A3, A4: ABAD-expressing SH-SY5Y, V1, V2: vector control HeLa transfectants, and V3, V4: vector control SH-SY5Y transfectants. Data are the mean \pm S.D. ($n=4$); * $p<0.05$ in ANOVA.

by ABAD against the exposure to ROS induced by treatment with antimycin A in HeLa and SH-SY5Y transfectants (Fig. 2B and C). It was reported that co-overexpression of ABAD and mutant APP induced cytotoxicity (Yan et al., 1997). In contrast to this report (Yan et al., 1997), no cytotoxic effect was observed even in the presence of A β without treatment with antimycin A (Fig. 2B and C). Only when cells were co-treated with A β and antimycin A, the difference between ABAD and control transfectants was evident. These findings indicate that A β suppresses the cytoprotective activity of ABAD to 4-HNE.

4. Discussion

ROS modifies unsaturated fatty acids to form peroxides, from which aldehydes such as malondialdehyde (MDA), and

highly toxic 4-HNE are non-enzymatically produced. 4-HNE has also been shown *in vitro* to promote neuronal death (Kruman and Mattson, 1999). Recently, marked increases in 4-HNE were reported in the hippocampus and superior and middle temporal gyrus of patients with mild cognitive impairment (MCI) and those with early AD compared with healthy individuals (Williams et al., 2006). 4-HNE not only induces neuronal death but also causes synapse dysfunction due to mechanisms such as reducing Na⁺, K⁺-ATPase activity (Pedersen et al., 1999) and markedly inhibits microtubule formation and neurite outgrowth (Neely et al., 1999). In this study, we demonstrated the role of ABAD in detoxification of *exogenous* and *endogenous* 4-HNE at cultured cell level, although it remains unclear whether ABAD actually functions to detoxify cytotoxic aldehydes in the brain.

ABAD has several functions: in the third step of mitochondrial fatty acid β -oxidation, as short chain 3-

hydroxyacyl-CoA dehydrogenase (SCHAD): additionally, ABAD catalyzed a wide spectrum of substrates, including steroids, cholic acids and fatty acid (Yang et al., 2005). Thus, if this multifunctional enzyme would have an additional function, it might be reasonable. When we pay attention on fatty acid β -oxidation (Schulz, 1991), the β -oxidation is not available in energy metabolism in the brain (Penicaud et al., 2006); however, ABAD, an enzyme involved in β -oxidation, expresses in the brain (Yang et al., 2005). Thus, it suggests that ABAD plays an alternative role in the brain instead of energy metabolism.

ABAD can detoxify 4-HNE only in the presence of NADH as a cofactor in the healthy brain according to our model. Thus, when energy metabolism to generate NADH is declined, the detoxification system by ABAD would not be functional, leading to amplifying toxic aldehydes. Since it is known that energy metabolism is poor in the brain of AD, NADH must be not abundant in AD brains. Moreover, in our model, A β plays a role toward the accumulation of 4-HNE by inhibiting the ABAD activity in the development of AD. Since 4-HNE stimulates the A β production (Tamagno et al., 2005), A β would in turn enhance to increase by 4-HNE. This vicious cycle could increase A β as well as 4-HNE, both of which should contribute to the pathogenesis of AD. Further study will be required to reveal the relationship between AD and ABAD.

Acknowledgments

This work was supported by grants from the Ministry of Health, Labour and Welfare (H17-Chouju-009, longevity science) to Shigeo Ohta.

Appendix A. Supplementary data

Supplementary data associated with this article can be found, in the online version, at doi:10.1016/j.neurobiolaging.2007.07.002.

References

- Burczynski, M.E., Sridhar, G.R., Palackal, N.T., Penning, T.M., 2001. The reactive oxygen species-and Michael acceptor-inducible human aldo-keto reductase AKR1C1 reduces the alpha,beta-unsaturated aldehyde 4-hydroxy-2-nonenal to 1,4-dihydroxy-2-nonenal. *J. Biol. Chem.* 276 (4), 2890–2897.
- Kruman, I.I., Mattson, M.P., 1999. Pivotal role of mitochondrial calcium uptake in neural cell apoptosis and necrosis. *J. Neurochem.* 72 (2), 529–540.
- Lustbader, J.W., Cirilli, M., Lin, C., Xu, H.W., Takuma, K., Wang, N., Caspersen, C., Chen, X., Pollak, S., Chaney, M., Trinchese, F., Liu, S., Gunn-Moore, F., Lue, L.F., Walker, D.G., Kuppusamy, P., Zewier, Z.L., Arancio, O., Stern, D., Yan, S.S., Wu, H., 2004. ABAD directly links Abeta to mitochondrial toxicity in Alzheimer's disease. *Science* 304 (5669), 448–452.
- Manczak, M., Anekonda, T.S., Henson, E., Park, B.S., Quinn, J., Reddy, P.H., 2006. Mitochondria is a direct site of A β accumulation in Alzheimer's disease neurons: implications for free radical generation and oxidative damage in disease progression. *Hum. Mol. Genet.* 15 (9), 1437–1449.
- Mark, R.J., Pang, Z., Geddes, J.W., Uchida, K., Mattson, M.P., 1997. Amyloid beta-peptide impairs glucose transport in hippocampal and cortical neurons: involvement of membrane lipid peroxidation. *J. Neurosci.* 17 (3), 1046–1054.
- Neely, M.D., Sidell, K.R., Graham, D.G., Montine, T.J., 1999. The lipid peroxidation product 4-hydroxynonenal inhibits neurite outgrowth, disrupts neuronal microtubules, and modifies cellular tubulin. *J. Neurochem.* 72 (6), 2323–2333.
- Ohsawa, I., Nishimaki, K., Yasuda, C., Kamino, K., Ohta, S., 2003. Deficiency in a mitochondrial aldehyde dehydrogenase increases vulnerability to oxidative stress in PC12 cells. *J. Neurochem.* 84 (5), 1110–1117.
- Ohta, S., 2003. A multi-functional organelle mitochondrion is involved in cell death, proliferation and disease. *Curr. Med. Chem.* 10 (23), 2485–2494.
- Pedersen, W.A., Cashman, N.R., Mattson, M.P., 1999. The lipid peroxidation product 4-hydroxynonenal impairs glutamate and glucose transport and choline acetyltransferase activity in NSC-19 motor neuron cells. *Exp. Neurol.* 155 (1), 1–10.
- Penicaud, L., Leloup, C., Fioramonti, X., Lorsignol, A., Benani, A., 2006. Brain glucose sensing: a subtle mechanism. *Curr. Opin. Clin. Nutr. Metab. Care* 9 (4), 458–462.
- Sayre, L.M., Zelasko, D.A., Harris, P.L., Perry, G., Salomon, R.G., Smith, M.A., 1997. 4-Hydroxynonenal-derived advanced lipid peroxidation end products are increased in Alzheimer's disease. *J. Neurochem.* 68 (5), 2092–2097.
- Selkoe, D.J., 1994. Alzheimer's disease: a central role for amyloid. *J. Neurobiol.* 53 (5), 438–447.
- Schulz, H., 1991. Beta oxidation of fatty acids. *Biochim. Biophys. Acta* 1081 (2), 109–120.
- Schulze-Osthoff, K., Bakker, A.C., Vanhaesebroeck, B., Beyaert, R., Jacob, W.A., Fiers, W., 1992. Cytotoxic activity of tumor necrosis factor is mediated by early damage of mitochondrial functions. Evidence for the involvement of mitochondrial radical generation. *J. Biol. Chem.* 267 (2), 5317–5323.
- Suzuki, Y., Fujisawa, M., Ando, F., Niino, N., Ohsawa, I., Shimokata, H., Ohta, S., 2004. Alcohol dehydrogenase two variant is associated with cerebral infarction and lacunae. *Neurology* 63 (9), 1711–1713.
- Tamagno, E., Parola, M., Bardini, P., Piccini, A., Borghi, R., Guglielmo, M., Santoro, G., Davit, A., Danni, O., Smith, M.A., Perry, G., Tabaton, M., 2005. Beta-site APP cleaving enzyme up-regulation induced by 4-hydroxynonenal is mediated by stress-activated protein kinases pathways. *J. Neurochem.* 92 (3), 628–636.
- Uchida, K., Stadtman, E.R., 1992. Modification of Histidine Residues in Proteins by Reaction with 4-Hydroxynonenal. *Proc. Nat. Acad. Sci. U.S.A.* 89 (10), 4544–4548.
- Williams, T.I., Lynn, B.C., Markesbery, W.R., Lovell, M.A., 2006. Increased levels of 4-hydroxynonenal and acrolein, neurotoxic markers of lipid peroxidation, in the brain in Mild Cognitive Impairment and early Alzheimer's disease. *Neurobiol. Aging* 27 (8), 1094–1099.
- Yan, S.D., Fu, J., Soto, C., Chen, X., Zhu, H., Al-Mohanna, F., Collison, K., Zhu, A., Stern, E., Saido, T., Tohyama, M., Ogawa, S., Roher, A., Stern, D., 1997. An intracellular protein that binds amyloid-beta peptide and mediates neurotoxicity in Alzheimer's disease. *Nature* 389 (6652), 689–695.
- Yang, S.Y., He, X.Y., Schulz, H., 2005. Multiple functions of type 10 17beta-hydroxysteroid dehydrogenase. *Trends Endocrinol. Metab.* 16 (4), 167–175.



Research Report

Involvement of mitoK_{ATP} channel in protective mechanisms of cerebral ischemic tolerance

Megumi Watanabe^{a,b}, Ken-ichiro Katsura^{a,*}, Ikuroh Ohsawa^b, Genki Mizukoshi^a,
Kumiko Takahashi^a, Sadamitsu Asoh^b, Shigeo Ohta^b, Yasuo Katayama^a

^aDivisions of Neurology, Nephrology, and Rheumatology, Department of Internal Medicine, Nippon Medical School, 1-1-5 Sendagi, Bunkyo-ku, Tokyo 113-8603, Japan

^bDepartment of Biochemistry and Cell Biology, Institute Of Development and Aging Sciences, Graduate School Of Medicine, Nippon Medical School, Japan

ARTICLE INFO

Article history:
Accepted 11 August 2008
Available online 26 August 2008

Keywords:
Ischemic tolerance
5-hydroxydecanoate
Diazoxide
Gerbil
Rat
Primary neuron
Mitochondrial KATP channel
Mitochondrial membrane potential

ABSTRACT

Little work has been performed to determine roles of mitochondrial ATP-sensitive potassium channels (mitoK_{ATP}) in ischemic preconditioning (IPC) in brain. To investigate the role on cerebral IPC, we examined effect of 5-hydroxydecanoate (5-HD), a selective mitoK_{ATP} blocker, and diazoxide (DZX), a selective mitoK_{ATP} opener on various IPC models. An IPC model with gerbil: 2 min bilateral common carotid arteries occlusion (BLCO) + 24 h recovery + 5 min BLCO. 5-HD, DZX, vehicle was administered 30 min before 5 min BLCO. Seven days later, surviving CA1 neurons were counted. A focal IPC model with rat: 15 min middle cerebral artery occlusion (MCAO) + 48 h recovery + 90 min MCAO. Twenty-four hours before 90 min MCAO, 5-HD, DZX, or vehicle was administered. One day after 90 min MCAO, neurological symptoms and infarct volumes were evaluated. An in vitro IPC model with primary neuronal cultures: 8 min oxygen–glucose deprivation (OGD) + 24 h recovery + 70 min OGD. Thirty minutes before 70 min OGD, 5-HD or DZX were added. One day later, surviving neurons were counted. Mitochondrial membrane potential was also monitored. 5-HD significantly attenuated the protective effect of IPC in gerbil model, rat model, and in vitro OGD model. DZX significantly facilitated the protective effect of IPC in gerbil and rat model. The mitochondrial membranes were depolarized with IPC, and 5-HD treatment significantly reduced this effect. These results strongly suggest that mitoK_{ATP} channel activation plays a key role in development of a protective mechanism of cerebral IPC.

© 2008 Elsevier B.V. All rights reserved.

1. Introduction

There is a continuous interest in understanding mechanisms of ischemic cell damage and in developing adequate treatments for stroke patients. It has been reported that ischemic tolerance (preconditioning) phenomenon, in which brief episodes of ischemia protect against subsequent lethal ischemia,

involves endogenous cellular protective mechanisms. This phenomenon has been observed in various animal models of forebrain ischemia (Kitagawa et al., 1990, Kirino, 2002, Heurteaux et al., 1995) and focal cerebral ischemia (Chen et al., 1996, Barone et al., 1998, Puisieux et al., 2000, Shimizu et al., 2001, Nakamura et al., 2002). It was also observed in human stroke patients that transient ischemic attack (TIA) could

* Corresponding author. Fax: +81 3 3822 4865.
E-mail address: k-katsur@nms.ac.jp (K. Katsura).

protect against subsequent final stroke damage (Wegener et al., 2004). Among the various mechanisms considered as mediators of preconditioning in brain, considerable attention has been drawn to the activation of adenosine A1 receptors and ATP-dependent potassium (K_{ATP}) channels. This study line was influenced by the report that both the K_{ATP} channel blocker glibenclamide and the A1 receptor antagonist DPCPX (1,3-dipropyl-8-cyclopentylxanthine) could abolish the protective effect of preconditioning in a rat global ischemia model when administered during the preconditioning insult (Heurteaux et al., 1995). However, recent study failed to support a direct involvement of A1 receptors or plasma membrane K_{ATP} channels during early stages in the development of ischemic tolerance in vivo (Sorimachi and Nowak, 2004), stating that the role of mito K_{ATP} channels remained to be elucidated. Activation of mitochondrial ATP-sensitive potassium (mito K_{ATP}) channels has been proposed to play a pivotal role in preconditioning (O'Rourke, 2000, Oldenburg et al., 2002) in heart. Pharmacological agents that open mito K_{ATP} channels showed preconditioning in heart (Garlid et al., 1997, Szewczyk and Wojtczak, 2002). Moreover, the physiological or chemical preconditioning phenomenon is prevented by selective mito K_{ATP} channel blockers (Horiguchi et al., 2003, Yoshida et al., 2004). The beneficial effects of mito K_{ATP} channel opener diazoxide have been also demonstrated in the heart (Garlid et al., 1997, O'Rourke, 2000, Oldenburg et al., 2002) and other organs (Kullin et al., 2003, Roth et al., 2006). However, in vivo experiments showing involvement of mito K_{ATP} channels in brain ischemic preconditioning were quite limited (Yoshida et al., 2004). Although they showed the cancellation of ischemic tolerance phenomenon by administration of mito K_{ATP} channel blocker 5-hydroxydecanoate (5-HD) in a rat MCAO model, because they administered 5-HD at 30 min before lethal ischemia, possibilities of direct effect of 5-HD itself still remain to be solved. In addition, we have published a report on the roles of adenosine receptors in ischemic tolerance phenomenon (Hiraide et al., 2001) and we were interested in clarifying the downstream signal transduction after adenosine receptor activation. To that end, we studied the roles of mito K_{ATP} channels in ischemic preconditioning by using mito K_{ATP} channel inhibitor 5-HD and mito K_{ATP} opener diazoxide (DZX) in a gerbil global ischemia model, rat transient middle cerebral artery occlusion (MCAO) model, and in vitro primary neuronal cell culture. Especially, in rat MCAO model, we administered 5-HD, or DZX at 24 h before the lethal ischemia (and 24 h after the preconditioning ischemia) to be free from the drug's direct effects on the lethal ischemia.

2. Results

2.1. Transient global ischemia with gerbil

Gerbil hippocampal CA1 neuronal densities after 5 min ischemia are shown in Fig. 1. Sham operation only showed neuronal densities of 187.3 ± 3.5 ($n=6$). Without preconditioning ischemia, 5 min of carotid occlusion decreased survival cells down to close to zero (5 min group). In the groups with 2 min preconditioning ischemia at 24 h before the 5 min ischemia, the decrease of the number of surviving cells was significantly

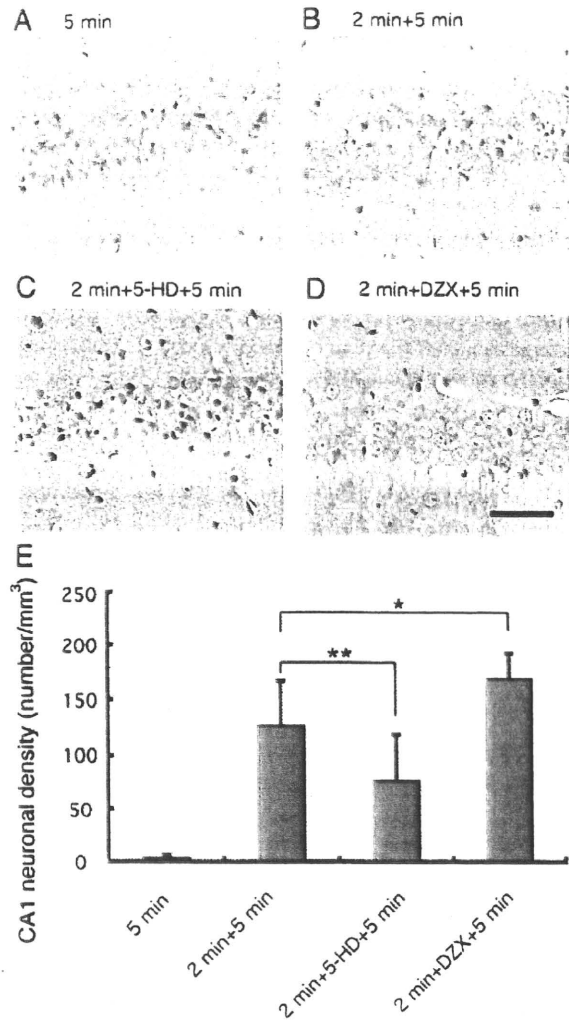


Fig. 1 – Five minutes of carotid artery occlusion gave rise to almost complete cell death (5 min; A). When 2 min ischemia was given 24 h before the 5 min ischemia (2 min + 5 min; B), the surviving neurons were significantly enhanced. The increase was significantly reduced when 5-HD was administered before the 5 min ischemia (2 min + 5HD + 5 min; C). The increase was significantly enhanced when DZX was administered before the 5 min ischemia (2 min + DZX + 5 min; D). Upper panels (A–D) showed typical histological appearances in gerbil hippocampus. Lower panel (E) showed CA1 neuronal densities. **: $p < 0.01$, *: $p < 0.05$. Scale bar in panel D shows 200 μ m.

attenuated after 5 min of carotid occlusion (2 min+5 min group). When 5-HD was administered intraperitoneally 30 min before 5 min occlusion (2 min + 5HD + 5 min group), the number of surviving neurons was significantly decreased compared to the number in the 2 min+5 min group. On the other hand, when DZX was administered 30 min before 5 min ischemia (2 min + DZX + 5 min group), the number of surviving neurons was significantly enhanced against the number of 2 min+5 min group.